Cover Crop Effects On Soil Hydrology

by

Rodolfo Bonilla

A thesis submitted to the Graduate Faculty of
Auburn University
in partial fulfillment of the
requirements for the Degree of
Master of Science

Auburn, Alabama
May 7, 2022

Keywords: Hydraulic Conductivity, Infiltration, Soil Water Retention, Cover Crops

Approved by

Thorsten Knappenberger, Chair, Associate Professor of Soil Physics
Joey N. Shaw, Professor of Soil Science
Audrey V. Gamble, Assistant Professor and Extension Specialist (Soil Science)

Abstract

Cover crops are known for their positive and significant effects on soils. They contribute to growing subsequent crops, reducing soil erosion, increasing water infiltration, and improving nutrient management. Cover crops can affect physical soil properties, such as infiltration, runoff, and water retention. These properties are influenced by soil structure, texture, soil organic matter, soil cover, soil water content, depth to the water table, and landscape features. The goal of this study was to determine the effect of three different cover crops, cereal rye (*Secale cereale*), crimson clover (*Trifolium incarnatum*), and radish (*Raphanus sativus*), on soil hydrology of Alabama soils. The objectives were to measure the saturated and unsaturated hydraulic conductivity at the soil surface and to determine the yield effects of cover crops on corn (*Zea mays*) and soybeans (*Glycine max* L.). A significant difference was found between seasons (spring and summer) and the hydraulic conductivity in the treatments ($P < 0.05$) for soybeans with saturated hydraulic conductivity. However, differences were not significant between seasons and the hydraulic conductivity for corn with saturated hydraulic conductivity. Also, a significant difference was found between seasons in soybean and corn ($P < 0.001$) for the unsaturated hydraulic conductivity in the treatments with the tension infiltrometer. There was no significant hydraulic conductivity and sorptivity difference between the crops using the ring infiltrometer method. The effects of cash crops on hydraulic conductivity appear to be stronger than the effects of cover crops during the growing season due to the root systems of the cash crops. ANOVA results showed that soybean yields were significantly higher for cover crop plots in 2020 ($P < 0.001$). For corn in 2020 and 2021, as well as for soybeans in 2021, there were no significant effects of cover crops on yield.

The second objective of this study was to estimate the soil hydrological properties with the BEST-2K method. This method utilizes saturated and unsaturated infiltration measurements together with the soil particle size distribution to estimate the soil water retention curve and the

hydraulic conductivity. Field experiments were conducted at two locations, the Old Rotation and a forest, on the Auburn University campus. Estimates from the BEST-2K method were compared to data measured with the HYPROP instrument. The HYPROP is used to measure the water retention curve and the unsaturated hydraulic conductivity of the soil. The BEST-2K method overestimated the volumetric water content of the water retention curve and the hydraulic conductivity for all samples. The root means square error (RSME) of the BEST-2K estimates and the HYPROP data were similar to the RSME of HYPROP field replicates. The BEST-2K method is helpful to estimate soil hydraulic properties when HYPROP instruments are not available.

Acknowledgments

First of all, I want to be thankful to God for letting me have this opportunity. Also, I would like to thank the Fulbright Organization for its scholarship program and for the opportunity to come to the United States to complete my master of science degree. I want to thank Auburn University for giving me admission and Dr. Thorsten Knappenberger for allowing me to work with him during these two years. I am thankful for my family, my parents, and my siblings for always supporting me. Thanks to all my friends and people I have met during my Fulbright experience, especially to the Gasperi-Jurado family, Gabriel Torres, Margaret Hamner, the McPherson family, Cory Johnson, Jhon Peter Dugaduga, Mayra Alejandra Paez, and finally but not least Cristina Gacho. To all of you, Thank you for your support.

Table of Contents

List of Figures

List of Tables

Chapter 1

Literature Review

1.1 Soil-Water Relationship

1.1.1 Capillary Action

Capillary is the ability of a liquid to move through small pores without any external force and against gravity (Beven & Germann, 2013; G. A. Clark & Smajstrla, 1993; Zhuang et al., 2019). The smaller the diameter of the pores, the higher the capillary will be. The capillary occurs as a result of the adhesion and cohesion forces against gravity. Water moves in soils for the capillary action through the network of the water molecules (Shukla, 2013). Soil properties such as porosity, texture, and water holding capacity, influence the capillary behavior (Jiang et al., 2019; Ludwig, Wilcox, Breshears, Tongway, & Imeson, 2005; Niemeyer, Fremier, Heinse, Chávez, & DeClerck, 2014). The capillary is the result of the hydraulic gradient in the interface between air and water. According to Shukla (2013), the capillary rise can be obtained through the following equation:

$$h = 2\gamma \cos \alpha / \rho g r \tag{1.1}$$

Where γ is the surface tension between the liquid and the air, α is the contact angle, ρ is the density of the liquid, g is the gravity, and r is the capillary radius.

1.1.2 Water Potential

Soil water potential is known as the potential energy found in the soil solution (Carter & Gregorich, 2007). The potential energy found in the soil solution will depend on the water chemical state (pure water, atmospheric pressure, temperature, and constant elevation) (Shukla, 2013). Water potential differences in the soil let the water moves from a higher water potential region to a lower water potential region. When the water potential is the same in the soil, that region is in an equilibrium state (no water flow). Water potential occurs by several physical factors such as gravity, mechanical pressure, and capillary action (Shukla, 2013). The total soil potential is the sum of the individual potentials:

$$\psi_T = \psi_g + \psi_m + \psi_o + \psi_a \tag{1.2}$$

where ψ_g gravimetric potential, ψ_m matric potential, ψ_o is the osmotic potential, and ψ_a is the gas potential.

The water potential can be expressed in three different ways; energy per unit mass (Jkg^{-1}), energy per unit volume (Jm^{-3} or kPa), and energy per unit weight (JN^{-1} or m, cm) (Hillel, 1998) The water potential can be measured by a tensiometer, heat dissipation sensors, and dewpoint potentiometer.

1.1.3 Soil Water Retention

Soil water retention is a fundamental soil property that affects infiltration, drainage, field capacity, plant available water, water stress on plants, and solute movement. Soil water retention is associated with the texture of the soil. Water attaches more to fine particles such as clay and loam for their capacity to retain water than larger sandy particles (Yang, Fan, & Jones, 2018). Soil water retention is affected by texture and soil organic matter (SOM) (Silva, Hashiguti, Zotarelli, Migliaccio, & Dukes, 2018). Water retention changes due to the texture of the soil that can retain

water (Yang et al., 2018). Soil water retention is typically described by a soil water retention curve (WRC).

The WRC describes the relationship between the soil matric potential ψ_m and the volumetric water content θ. The WRC can be considered one of the most important properties of soil hydrology. It expresses the equilibrium between the soil volumetric water content and the matric potential (Alsherif, Wayllace, & Lu, 2015). Many soil water retention curve empirical models are used to describe the movement of water in the soil. Brooks-Corey, Campbell, and van Genuchten are some of the models that are used to calculate the water retention curve (Jarosław Kaszubkiewicz, 2015; Lenhard, Parker, & Mishra, 1989; Sommer & Stöckle, 2010). WRC can be expressed in two different ways: as tension which is a positive measure, and as matric potential, which is a negative measure (Alsherif et al., 2015).

1.1.4 Field Capacity

The field capacity refers to the water a soil can hold against gravity (Basche & DeLonge, 2017). Field capacity is correlated positively with the total porosity (Jiang et al., 2020). Generally, the field capacity is obtained in the laboratory by equilibrating a soil sample to a certain matric potential. For sandy soils, the field capacity is the volumetric water content at a matric potential of $\psi_m = -10\,kPa$, and for fine-textured soils, it is the volumetric water content at a matric potential of $\psi_m = -33\,kPa$.

1.1.5 Plant Available Water

Plant available water (PAW) is known as the volumetric water content between field capacity and the permanent wilting point. The permanent wilting point is the volumetric water content θ_{PWP} found at a matric potential of $\psi_m = -1,500\,kPa$. At this matric potential, plants will permanently wilt. Plant available water is highest for loamy soils, followed by clayey and sandy soils.

1.1.6 Water Storage

Water storage in the soil is the amount of water retained in the soil after precipitation. Water storage is an important property to consider in hydrological studies. Water storage can vary depending on the soil's physical conditions. Soil water storage is higher in soils under cover crops (Chalise et al., 2018). Cover crops are known for improving the water storage in soils (Chalise et al., 2018). Water storage is associated with water infiltration processes through soil (Jiang et al., 2017). Infiltration helps to reduce water surface runoff and erosion risk and improves water storage (Zhu et al., 2019).

1.2 Soil Hydrology

Soils are an essential part of the hydrologic cycle. Hydrologic processes such as infiltration and water flux determine the water movement in soils. Soil hydrology describes the movement of water in saturated or unsaturated soils (Hinnell, Lazarovitch, & Warrick, 2009). The movement of the water in soils is a complex process that changes over time (Nofziger & Wu, 2000). The knowledge of water movement in soils helps to understand other processes occurring in soil hydrology (Nofziger & Wu, 2000).

1.2.1 Infiltration

Infiltration is the process of water entering the soil surface due to rainfall or irrigation. Generally, the infiltration rate is higher at the beginning and then decreases with time (Nofziger & Wu, 2000). Soil properties, such as soil structure, texture, soil organic matter, and water content, affect the infiltration process of the soil (Haruna & Nkongolo, 2015). Soil physical characteristics such as texture, structure, and bulk density, can be indicators for the infiltration in the soil (Alaoui, Caduff, Gerke, & Weingartner, 2011; Bargués Tobella et al., 2014; Castellano & Valone, 2007). The infiltration rate is lower in soils with silty and clay textures; in consequence, the retention of water is higher than in sandy soils (Yang et al., 2018). Infiltration data obtained from the

unsaturated and saturated soil profiles improve the study of the hydraulic conductivity in the field (Hinnell et al., 2009). Water infiltration forms the link between surface and subsurface hydrology.

Saturated Infiltration

Saturated soil is an infiltration condition where all soil pores in the soil are filled with water. Saturated soils are studied for their contribution to describing the movement of water and solutes in the soil (Jačka, Pavlásek, Kuráž, & Pech, 2014; Reynolds, Bowman, Brunke, Drury, & Tan, 2000). An infiltrometer is an instrument used *in situ* for measuring the movement of liquid into the soil (Rönnqvist, 2018). There are many instruments to measure saturated infiltration. The single or double ring infiltrometer test is the most used method to measure saturated infiltration. The steady infiltration rate can be affected by the ring infiltrometer dimensions, the matric potential at the wetting front, ring depth, soil porosity, and capillarity (Fatehnia, Tawfiq, & Ye, 2016). The infiltration rate is obtained through a measured volume of water added inside the ring infiltrometer to keep a constant level (Fatehnia et al., 2016). The volume of water used during each measured time interval should be converted into the depth of water per unit of time (e.g., centimeters per hour). Infiltration is measured until the infiltration rate becomes constant.

Unsaturated Infiltration

Unsaturated soils are known for having soil pores filled with water and air. Unsaturated soils are described by the unsaturated hydraulic conductivity and the volumetric water content. Infiltration of water into unsaturated soils can occur in the form of fingers for certain reasons, and the water movement is faster in unsaturated soils than in saturated soils (Zhu et al., 2019). A tension infiltrometer is a device used to measure the hydraulic properties of unsaturated soils. A tension infiltrometer lets the water move at a slower rate than water found free on the surface. This is possible due to the negative water pressure coming out from the disk of the infiltrometer into the soil. The more negative water pressure applied, the more soil pores would be without water (unhydrated), and the more unsaturated the soil would be.

1.3 Soil Properties Affecting Soil Hydrology

Soil particles and their distribution

There is a wide variety of soil particles; soil scientists classify soil particles according to their sizes into sand, silt, and clay. Clay particles are smaller than $0.002\,mm$ in diameter. Silt particles are from 0.002 to $0.05\,mm$ in diameter, and sand ranges from 0.05 to $2.0\,mm$. Particles larger than $2.0\,mm$ are classified as gravel or stones. There are 12 USDA soil textural classes represented on the soil texture triangle. Soil particles are important for the formation of soil structure. The particle size distribution is a representation of the percentage of soil particles found in soil samples. Soil particle distribution plays an important role in the soil hydrology cycle (G. A. Clark & Smajstrla, 1993).

1.3.1 Soil Structure

The congregation of soil particles is known as soil structure. Larger aggregates are formed due to the union of single particles. Different soil structures are established during the aggregation of the soil particles. The USDA classifies the soil structure into seven classes; granular, platy, prismatic, columnar, lenticular, wedge, and blocky. There are also structureless conditions classified as single grain and massive. The plant growth, aeration, and water movement in the soil will depend on the soil structure. A good soil structure will increase the infiltration rate and improve drainage. Structureless soils present several problems such as anaerobic activity, nutrient loss, and erosion. Soil hydrology processes will depend on the soil structure. Many physical and chemical processes in the soil are linked to the soil structure (Jiang et al., 2018). Soil structure and other internal factors (physicochemical factors) could modify the soil water infiltration rate (Bond & Harris, 1964; Czarnes, Hallett, Bengough, & Young, 2000).

Porosity

Soil porosity is also known as pore space and is the void space in soil that can be filled with water or air. Soils of good quality have large pores that are used for the circulation of air, water, and nutrients that plants obtain through the root systems. Porosity is affected by the structure and texture of the soil. Porosity can be increased by microbiological activity and the root system of plants (Ludwig et al., 2005; Zhu et al., 2019). Benegas, Ilstedt, Roupsard, Jones, and Malmer (2014) reported that "tree roots (living and decaying) affect in a positive way soil infiltration by increasing macroporosity and soil aggregation." Porosity is related to good hydrology conditions in the soil (Jiang et al., 2020).

Bulk Density

Bulk density is the dry weight of soil in a given volume. High bulk density can be found in compacted soils. Plant root growth is limited in soils with a high bulk density. Soils with sandy textures are more exposed to having a high bulk density Infiltration can be reduced by high bulk density in the soils (Jiang et al., 2020). Root development during plant growth influences the bulk density of the soil (Jiang et al., 2018). According to Hubbard, Strickland, and Phatak (2013), "bulk density values in the crop rows are significantly lower than values in the interiors." Soils with a high percentage of organic matter and pore spaces have lower bulk density.

1.4 Soil Hydraulic Properties

The movement of water in the soil is influenced by soil physical characteristics and the hydrology parameters (Šimůnek, van Genuchten, & Wendroth, 1998). Some soil physical characteristics can be easily determined by the soil hydraulic properties, such as infiltration, water retention, available water capacity, and hydraulic conductivity (Rousseva et al., 2017). Hydraulic properties refer to the capacity of soil to transmit water in different conditions (Carter & Gregorich, 2007).

1.4.1 Hydraulic Conductivity

The hydraulic conductivity (K) is the capacity of soil to move and distribute the water in saturated conditions (Zwartendijk et al., 2017). The hydraulic conductivity is influenced by soil morphological features such as texture, soil organic matter, and bulk density (Saxton & Rawls, 2006). The hydraulic conductivity changes depending on field conditions and physical properties (Reynolds et al., 2000). In general, soil texture, particle density, bulk density, and porosity are the factors affecting hydraulic conductivity the most. Other factors such as chemical properties have insignificant effects. Hydraulic conductivities in sandy soils are relatively high (Hubbard et al., 2013) The infiltration of water into the soil depends on the soil hydraulic conductivity (Ludwig et al., 2005).

Soil hydraulic conductivity is determined *in situ* to understand the soil hydrologic processes (Bouma, 1981). The hydraulic conductivity is different in soils with crops than in soil without any vegetation. Hydraulic conductivity is greater in the crop rows than in the inter rows. It means that a greater portion of water may infiltrate in the row and be directly available to plants than the water which falls on the inter rows (Benegas et al., 2014; Hubbard et al., 2013; Jiang et al., 2019; Zhu et al., 2019). The hydraulic conductivity exhibits a high spatial heterogeneity. Crops have a positive impact on soil hydraulic properties, with higher infiltrability and hydraulic conductivity (Zhu et al., 2019). Hydraulic conductivity is calculated by Darcy and Richards equations.

In the study of the movement of water in the soil, the determination of the hydraulic conductivity and the infiltration capacity is very important, and the most used methods are the following: constant head permeameter, Saturo, single and double ring infiltrometers, tension infiltrometer, and rainfall simulators.

For saturated hydraulic conductivity, the single or double ring infiltrometer is used. This method is inexpensive and easy to use. The Saturo (Meter Group, Pullman, WA, USA) instrument can also be applied. The Saturo measures the permeability and field saturated hydraulic conductivity (K_{fs}) in soil, reducing error in the assessment and giving a rapid measurement.

To measure the unsaturated hydraulic conductivity, a tension infiltrometer is used. The SMS tension infiltrometer (Soil Measurement Systems, Tucson, Az, USA) measures the unsaturated

flow of water into soil in a fast and facile way. The data obtained by the saturated and unsaturated conductivities and water retention characteristics is important to estimate the water movement in the soil (Katsura, Kosugi, Yamamoto, & Mizuyama, 2006). The estimation of the hydraulic conductivity in soils can be demonstrated by Campbell's model.

1.4.2 Sorptivity

Sorptivity is one of the hydraulic properties (Carter & Gregorich, 2007). It reflects the capacity of soil to absorb water by capillarity (Haruna, Nkongolo, Anderson, Eivazi, & Zaibon, 2018). Sorptivity is related to hydraulic conductivity properties(Schulte, Culligan, & Germaine, 2007).

1.5 Water Movement and Distribution

The movement of the water occurs in different ways and requires different observations (Gowdish & Muñoz-Carpena, 2018). The water movement and distribution in a soil profile will depend on the texture of the soil (Yang et al., 2018). Good knowledge of the water movement is important to have better management of water resources (Nofziger & Wu, 2000). Water moves from areas of high soil water potential levels to areas of lower soil water potential. However, water can move in different directions (Nofziger & Wu, 2000). Redistribution of the water can occur for the differences in the hydraulic conductivity in soils (Zhu et al., 2019).

The Darcy-Buckingham law can be applied to describe the water movement in soils (Clothier, Sauer, & Scotter, 1991). Previous experimental work let Buckingham obtain a single formula to describe the saturated and unsaturated flow in soil:

$$q = -K(\theta)\frac{d(\psi_m + \psi_g)}{d_z} \tag{1.3}$$

Where $K(\theta)$ is the hydraulic conductivity as a function of the soil volumetric water content and $d(\psi_p + \psi_g)/d_Z$ is the gradient of the hydraulic potential in the z-direction. This formula is a generalization of Darcy's Law.

1.5.1 Soil Water Flow

Soil water flow depends on the potential of the water in saturated and unsaturated conditions (Silva et al., 2018). The movement of water through pores in the soil is under the unsaturated hydraulic conductivity control, and it is influenced by soil physic characteristics (Saxton & Rawls, 2006). According to Jiang et al. (2020), "the accurate translation of water flow behaviors such as the matrix flow, preferential flow, and lateral flow, helps the people understand rainwater redistribution (surface runoff, rainfall infiltration, plant water store, and groundwater recharge)." Soil water flow varies according to the flow speeds in soil pores. Water flow varieties differently between zones with or without roots (Ludwig et al., 2005; Niemeyer et al., 2014). Water table and rainfall events modify the soil water flow (Silva et al., 2018). Water movement in different soil layers depends on the length and conductivity of each soil layer (Nofziger & Wu, 2000). The categorization of the different flows (saturated flow, unsaturated flow, and water vapor movement) in the soil is important to understanding the infiltration regimes (Weiler & Flühler, 2004). Soil water can move through the soil matrix or preferentially along with the soil structure and between soil aggregates.

Matrix Flow

Matrix flow is known for its even movement of water in the micropores in the soil (Weiler & Flühler, 2004). Matrix flow shows the water concentration of the drain. According to Cullum (2009) "matrix porosity (matrix flow) was defined as that porosity carrying water and solutes slowly enough, so there is extensive mixing between pores, consistent to Darcy's law and for solute transport by the convective dispersive equation." Matrix flow varies according to the physical properties of the soil and the presence of root plants (Ludwig et al., 2005; Niemeyer et al., 2014). The matrix flow can be measured in the field through a tension infiltrometer (Lassabatère et al., 2019).

Lateral Flow

Lateral flow is known as the movement of water in a lateral direction (Ritsema & Dekker, 1995; Wine, Ochsner, Sutradhar, & Pepin, 2012). Lateral flow can be modified by such a response of the microclimate and hydrological processes by vegetation (Bargués Tobella et al., 2014; Benegas et al., 2014). Several factors affect the lateral flow, such as; low permeability in the layer, the different permeabilities of water in the different horizons of the soil, the characteristics of rainfall events, the capacity of the soil to store water, and the slope of the surface and layers of the soil. The improvement of lateral flow benefits the distribution and water movement in the soil and helps plants to obtain water in dry seasons Zhu2019. Lateral root systems improve the movement of water in lateral directions and the interchange of water in the soil matrix (Zhu et al., 2019).

Preferential Flow

According to Beven and Germann (2013), "preferential flow is known as the process by which water moves unevenly through soils with a preferred track more preferably than uniform flow." Also, according to Hendrickx and Flury (2001), "preferential flow is defined as the movement of water and solutes through defined trackways while bypassing a fraction of the matrix pore." Preferential flow can be classified in different scales (Jiang et al., 2020). Preferential flow tracks show more microbial activity than the rest of the soil (Bundt, Widmer, Pesaro, Zeyer, & Blaser, 2001). Preferential flow is an important topic of research to understand the soil water flow (Jiang et al., 2020). Moreover, preferential flow trackways can change according to the soil physical characteristics and vegetation (Beven & Germann, 2013; Jiang et al., 2020).

In saturated soil, the preferential flow includes the fast movement of water from macropores. In unsaturated soil, preferential flow occurs, followed by lateral absorption (Bouma, 1981). According to Bouma (1981), "preferential flow in macropores can be filled by unlined boreholes when these end inside (unsaturated) peds." The increment of the infiltration and the preferential flow have a beneficial effect on reducing water runoff by generating infiltration in the area between

rows(Zhu et al., 2019). Preferential flow depends on the limitation of the time and the magnitude of inputs (Beven & Germann, 2013).

Preferential flow can be approached in four ways. These are 1. the single continuum perspective where preferential flows are studied by conductivity curve to a saturation point. 2. double continuum perspective where one domain is treated as immobile, and the other is treated as a domain by the Darcy-Richards equation; 3. double permeability approach where preferential flows are shown by high permeability including a Darcy-Richards domain; and 4. a double porosity approach where simple volume filling is used for the preferential flows (Beven & Germann, 2013).

Preferential flow paths have more tendency to dry and wet than the soil matrix. The transport of chemicals and substances in the preferential flow paths is higher than in the soil matrix (Bundt et al., 2001; Kahl, Fernandez, Rustad, & Peckenham, 1996). Preferential flow paths have excellent conditions for microorganisms. Therefore, preferential flow tracks can be interpreted as the continuous volatile situation in soils. Physicochemical properties in the preferential flow tracks are unique and distinct from those of the soil matrix. According to Bundt, Albrecht, Froidevaux, Blaser, and Flühler (2000), "gradients between preferential flow paths and soil matrix can be formed because the preferential flow paths have been persistent for decades." Lateral flow, together with homogeneous infiltration and wetting front instabilities, produce preferential flow in soils (Allaire, Roulier, & Cessna, 2009; Bundt et al., 2001). The transformation from preferential vertical flow to preferential lateral flow in the soil profile depends on the soil morphology characteristics (Beven & Germann, 2013).

Finger flow is the most common type of preferential flow (De Rooij, 2000). The water in finger flow moves irregularly through non-uniform ways as fingers (Rezanezhad, Vogel, & Roth, 2006). The infiltration and water distribution in the soil are impacted by the finger flow. This phenomenon can happen in homogeneous soils and well-structured soils as well (Ritsema et al., 1997). Finger flows are formed by heterogeneity or instability. Finger flow can be seen in clay soils with an adequate network structure (X. Wang et al., 2018). Fingers in sandy loam soils formed fast and at higher soil water retention (X. Wang et al., 2018).

1.6 Cover Crops and Their Effects on Soil Hydrology

Cover crops have a big influence on improving soil quality. They offer several benefits such as soil loss control, increased water infiltration, and increased nutrients in the soil (Haruna & Nkongolo, 2015). Nowadays, more farmers are interested in keeping crop residue and applying cover crops (CC) (Johnson, Strock, Tallaksen, & Reese, 2016). Cover crops are known for their contribution to increasing soil morphology characteristics. The incorporation of cover crops impacts the soil microbiological activity and the accessibility of nutrients to subsequent crops (De Baets, Poesen, Meersmans, & Serlet, 2011). Cover crops provide minerals and nutrients to the soil that can be taken up by microorganisms and plants (De Baets et al., 2011). Cover crops improve soil hydrological properties in the soil such as infiltration and hydraulic conductivity. Cover crops improve soil's physical properties such as texture, structure, and porosity that influence the infiltration, water runoff, and water retention in the soil for crop growth (Auler, Miara, Pires, Fonseca, & Barth, 2014; Blanco-Canqui, Mikha, Presley, & Claassen, 2011; Hubbard et al., 2013). According to Haruna et al. (2018),"the hydraulic conductivity parameter value determined from cover crops is about 75 percent greater than that for fields with no cover crops." The root system of the cover crops modifies some soil physical properties like the infiltration and the water flow in the soil (Jiang et al., 2018). Water is the most limited natural resource in agricultural production. Conservation farming techniques like cover crops help to improve the water infiltration into the soil (Haruna et al., 2018). The capacity of cover crops to enhance the water infiltration can decrease the surface runoff and nutrient loss and improve the yield of crops (Haruna et al., 2018; Ludwig et al., 2005). Cover crops are known to improve infiltration rates and saturated hydraulic conductivity (Haruna et al., 2018; Niemeyer et al., 2014). Also, cover crops change the porosity of soils, and results can be seen in increased saturated and unsaturated soil hydraulic conductivity. One of the theories for the higher infiltration in cover crops is related to the improvement of the micro and macropores in the soil, the channels formed by the roots of the plants, and the soil with higher porosity (Chalise et al., 2018). Cover crops biomass has a significant effect on soil moisture (Daigh et al., 2014).

Cover crops affect soil fertility by adding organic matter and nitrogen and avoiding nutrient loss (Haruna & Nkongolo, 2015). Cover crops residues help to increase some nutrients in the soil and be available for the next cash crop. Cover crops are applied as erosion control and environmental conservation technique in regions with extreme environmental conditions. Basche and DeLonge (2017) showed that the adoption of cover crops for more than ten years improved soil hydrological properties such as total porosity and water retained at field capacity. Management practices like cover crops that help improve physical soil conditions are encouraged (Haruna et al., 2018).

1.6.1 Effects of Plant Roots

The root morphology of the plants can affect the water movement and distribution in soil (Jiang et al., 2018). This movement varies in the different layers and horizons of the soil in the direction of the root (Jiang et al., 2018). Roots modify and influence water infiltration (Jiang et al., 2018). Root channels that have been opened by the presence of plants have increased the macroporosity in soils (R. Wang & Strong, 1996). Roots improve soil physical properties in several distinct ways (Ghestem, Sidle, & Stokes, 2011). The space created by roots can provide and be used for water and air storage in soil (Jiang et al., 2018). According to Jiang et al. (2018), "during root penetration, soil particles reorganize around the surface of the root to form a root channel and affect bulk density, non-capillary porosity, infiltration time, and hydraulic conductivity." Root channels created by previous crops can influence the root growth direction of new plants (Hinsinger, Bengough, Vetterlein, & Young, 2009). Roots provide the circulation of water in different phases between the lithosphere and the atmosphere. According to Hinsinger et al. (2009), "water lost through stomata during photosynthesis has to be replaced by uptake from the soil."

1.7 Estimation of Soil Hydraulic Parameters Using The BEST Method

BEST – Also known as Beerkan Estimation of Soil Transfer parameters incorporate pedotransfer functions to estimate the soil hydraulic parameters with water infiltration measurement yielding the scale specification of these curves (Angulo-Jaramillo et al., 2019). The BEST method of soil

hydraulic characteristics, developed by Lassabatère et al. (2006), provides the double estimation of the soil water retention and hydraulic conductivity curves by soil physical characteristics data that includes soil bulk density, particle-size distribution of the soil, cumulative three-dimensional infiltration, and the soil water content at the beginning and end of the infiltration readings (Angulo-Jaramillo et al., 2019).

According to Hillel (1998), "soil hydraulic properties are important to understand the transmission properties and water balance in the soil." Shape parameters from particle-size distribution analysis and parameters obtained from infiltration experiments can be estimated by the BEST method at the null pressure head. At the end of the infiltration readings, saturated water content is measured. Steady-state infiltration rate and the estimation of sorptivity (S) provide the information to estimate the hydraulic conductivity and the water retention curve. According to Lassabatère et al. (2006), "this is provided by fitting transient infiltration data on the classical two-term equations with values from zero to a maximum corresponding to null hydraulic conductivity and using a data subset for which the two-term infiltration equations are verified as valid."

BEST-1K

BEST-1K is derived from the initial method known as BEST, and it is used to recuperate water retention and hydraulic conductivity from the soil particle size distribution, saturated water content, initial water content, and accumulative infiltration from a single metal ring infiltrometer. BEST-1K only fits ring infiltrometer data, and there are three methods named BEST-1K slope, intercept, and steady (Lassabatère et al., 2019). Table 1.1 shows an overview of the three methods.

BEST-2K

BEST-2K is an extended method from BEST-1K, which also includes unsaturated infiltration measurements and is capable of estimating the soil hydraulic properties of a bimodal soil (Lassabatère et al., 2019). The infiltration is measured when pores in the matrix and fast-flow regions are completely activated (Lassabatère et al., 2019). BEST-2K inputs include two experiments for the water

Table 1.1: The BEST-1K main differences between the Best-Slope, Best-Intercept, and Best-Steady.

Best - Slope	**Best - Intercept**	**Best - Steady**
Developed in 2006.	Developed in 2010.	Developed in 2014.
Has a higher chance not to give positive estimates of sorptivity and hydraulic conductivity.	Gives positive estimates of sorptivity and hydraulic conductivity.	Combines procedure of best slope and intercept.
Failed frequently.	Rarely failed.	Describe the steady state of the infiltration.
Must be applied first and then if it failed, apply Best - intercept.	Must be applied in case of Best - slope failure.	Should be considered a promising alternative to analyze the ring infiltrometer data.

infiltration: a metal ring infiltration observation to calculate the cumulative bulk water infiltration and a tension infiltrometer reading performed at a high pressure to calculate the cumulative infiltration into the matrix alone. Other inputs include soil physical characteristics such as the initial water content before the infiltration readings for the two experiments, the water content of the tension infiltrometer at the end of the observations, the bulk density obtained from the saturated water content, and the soil particle size distribution (Lassabatère et al., 2019).

1.8 Research Objectives

The rationale of this study was based on knowing the benefits of the cover crops, how they can impact on the cash crops, and soil hydrology behavior. The main objective of the research was to evaluate the impact of different cover crops on soil hydrology in Alabama and their impact on the yield of cash crops. The second objective was to estimate the hydraulic conductivity in the cover crops and different areas in Alabama by the BEST-1K and the BEST-2K methods.

Chapter 2

Effects of Cover Crops on Water Infiltrability and Yield

2.1 Abstract

Cover crops are known for their positive and significant effects on soils. They contribute to growing subsequent crops, reducing soil erosion, increasing water infiltration, and improving nutrient management. Cover crops can affect physical soil properties, such as infiltration, runoff, and water retention. These properties are influenced by soil structure, texture, soil organic matter, soil cover, soil water content, depth to the water table, and landscape features. The goal of this study was to determine the effect of three different cover crops, cereal rye (*Secale cereale*), crimson clover (*Trifolium incarnatum*), and radish (*Raphanus sativus*), on soil hydrology of Alabama Compass and Marving soil series. The objectives were to measure the saturated and unsaturated hydraulic conductivity at the soil surface through infiltration and to determine the yield effects of cover crops on corn (*Zea mays*) and soybeans (*Glycine max* L.). A significant difference was found between seasons (spring and summer) and the hydraulic conductivity in the treatments ($P < 0.05$) for soybeans with Ksat. However, differences were not significant between seasons and the hydraulic conductivity for corn with Ksat. Also, a significant difference was found between seasons in soybean and corn ($P < 0.001$) for the unsaturated hydraulic conductivity in the treatments with the tension infiltrometer. There was no significant hydraulic conductivity and sorptivity difference between the crops using the ring infiltrometer. The effects of cash crops on hydraulic conductivity appear to be stronger than the effects of cover crops during the growing season due to the root systems of the cash crops. ANOVA results showed that soybean yields were significantly higher

for cover crop plots in 2020 ($P < 0.001$). For corn in 2020 and 2021, as well as for soybeans in 2021, there were no significant effects of cover crops on yield.

2.2 Introduction

The soil physical properties and processes of agricultural fields, such as infiltration, water surface runoff, and soil water retention, are important for crop growth (Hubbard et al., 2013). Soil physical characteristic properties such as infiltrability and water flow behavior are closely associated with cover crops root morphology (Jiang et al., 2018). Water is usually the most limiting factor in agricultural grain crop production. Agricultural management practices, such as cover crops, play a role in water infiltration into soil (Haruna et al., 2018). The ability of cover crops to improve the water movement in the soil can lead to reduced water surface runoff, nutrient loss, and increased crop productivity (Haruna et al., 2018). Cover crops improve soil structure by adding organic matter and creating soil pores providing better conditions to form aggregate and increasing the infiltrability of the soil (Ludwig et al., 2005).

Cover crops are known to increase infiltration rates and saturated hydraulic conductivity (A. Clark, 2015; Niemeyer et al., 2014). Also, cover crops change the pore size of soils, and results can be seen in the saturated or unsaturated soil hydraulic conductivity. Researchers have found that cover crops can increase infiltration and yield as well (A. Clark, 2015; Haruna et al., 2018; Niemeyer et al., 2014). The yield benefit can be distinguished after three to five years of using cover crops (Snapp et al., 2005). Farmers will start to see other benefits, such as soil health improvement and more microbial activity, after several years of including cover crops in their crop rotation (Snapp et al., 2005). Several factors are likely to have contributed to sustained gains in yield: fertilizer application, irrigation, increased soil tillage, and improved farming practices. For example, cover crops have been demonstrated to increase crop production, add organic matter to the soil, improve the porosity of the soil, increase the microbiology and biodiversity in the soil, and decrease erosion percentage (Snapp et al., 2005). There is evidence that applying cover crops increases protection from intensive rainfall.

Cover crops are less expensive than other agriculture practices such as livestock, dairy farming, and grain farming and have the potential to produce long-term benefits. However, cover crop costs can vary depending on the farm and the equipment needed. The cost of establishing cover crops can vary widely depending on the seeds, plant species, the area to establish the cover crops, and the technique applied to plant (Snapp et al., 2005). If the cover crops used are deeper rooting, they create macropores that increase the ability of air and water to penetrate the soil (Villamil, Bollero, Darmody, Simmons, & Bullock, 2006).

The rationale of this study was based on knowing the benefits of the cover crops, their impact of them on the cash crops, and soil hydrology behavior. Soil hydrology is known as an indicator of several soil properties. Due to the climate change, soil erosion, and lack of information on the cover crops' effects in Alabama, studying the impact of the cover crops on the soil hydrology and the hydraulic conductivity is important to have better management of this technique and soil-water natural resources.

The goal of this study was to determine the effects of cover crops on soil hydrology. Specific objectives of this research were to: 1. Determine the effects of cover crops on soil hydraulic conductivity and crop yield for corn and soybeans. 2. Evaluate the BEST-1K method to estimate soil hydraulic conductivity of cover crop soils.

2.3 Material and Methods

2.3.1 Project Site: E.V. Smith Research Center

The E.V. Smith Research Center (EVSRC) was established in 1978 by Auburn University with an area of 1544 ha (latitude 32.44197°, longitude, -85.89774°, and elevation 67.40 meters). The EVSRC has research units dedicated to dairy cattle, beef cattle, horticulture, plant breeding, field crops, and biosystems engineering. Research areas include certified organic vegetable production and conservation tillage. The predominant soils for the sites at EVSRC consist of Compass (Coarse-loamy, siliceous, subactive, thermic Plinthic Paleudults) and Marvyn (Fine-loamy, kaolinitic, thermic Typic Kanhapludults) soil series; however, in the area of the project, the soil

was loamy sand with a 1 to 3 percent slope. The mean annual precipitation is $1359\ mm$. The mean annual air temperature is 17 degrees Celsius.

2.3.2 Methodology and Experimental Design

Two areas at the EVSRC field crops unit were selected (Figure 2.1) and (Figure 2.2) with four replicates and twelve cover crops plots, each one with the following dimensions 3.7m x 12m (12 x 40 feet). In each replicate, four treatments were selected (fallow, cereal rye, crimson clover, and radish) in both areas (southeast and southwest) (Table 2.1). There was a fallow plot for each replicate to compare the results with the cover crop plots. In each plot, 1x2 meter subplots were established to evaluate the infiltration and hydraulic conductivity. The infiltration and hydraulic conductivity were measured in two seasons, during spring and summer of 2020. In each season, the infiltration was taken in the row of the cash crop.

Cover crop plots were established for the first time during the 2016 growing season, and they have been planted every year since then. During the spring, infiltration measurements in the plots were either fallow, or planted with cover crops (cereal rye (*Secale cereale*), crimson clover (*Trifolium incarnatum*), and radish (*Raphanus sativus*)). During the summer, the infiltration measurements were in the cash crops (corn (*Zea mays*) (southeast), and soybeans (*Glycine max* L.) (southwest)) planted in the plots (treatments from one to four) (Figure 2.3). Cash crop yields were measured in all the 12 plots with different treatments during 2020 and 2021.

In 2020, corn was planted on April 9 and harvested on August 21, 2020. The corn variety was DKC 62-08 SS. 80,000 seeds/ha (32,000 seeds/A) was planted at a depth of $3.80\,cm$ with a row spacing at $91\,cm$. Corn received three rounds of fertilization (one round $266\,kg/ha$ fertilizer $17-17-17$ and two rounds $112.25\,kg/ha$ fertilizer $28-0-0-5$) and nine irrigation events ($157.48\,mm$) during the growth season. Soybeans were planted on June 9 and harvested on November 4, 2020. The soybean variety was P76T54R2, and it was planted at a rate of 340,000 seeds/ha (10.7 seeds/ft), planted at a depth of $1.90\,cm$ with a row spacing at $91\,cm$. Soybean received two rounds of fertilization ($78.92\,kg/ha$ fertilizer $0-46-0$ and $150.22\,kg/ha$ fertilizer $0-0-60$) and

Figure 2.1: The southeast research area which was planted with corn in 2020 and soybeans in 2021.

Figure 2.2: The southwest research area which was planted with soybeans in 2020 and corn in 2021.

Figure 2.3: Crops from left to right; radish (*Raphanus sativus*), cereal rye (*Secale cereale*), crimson clover (*Trifolium incarnatum*), corn (*Zea mays*), and soybeans (*Glycine max* L.).

Table 2.1: Treatments with one, two, and three different species as cover crops. Numbers in parenthesis indicate the range of seeds planted per each species (kg/ha) .

	Number of Species		
Trt	**1**	**2**	**3**
1	Fallow		
2	Cereal rye (90)		
3	Crimson clover (20)		
4	Radish (8)		
5	Cereal rye (45)	Crimson clover (20)	
6	Cereal rye (30)	Crimson clover (20)	
7	Cereal rye (45)	Radish (8)	
8	Cereal rye (30)	Radish (8)	
9	Crimson clover (20)	Radish (8)	
10	Crimson clover (10)	Radish (8)	
11	Cereal rye (45)	Crimson clover (10)	Radish (4)
12	Cereal rye (30)	Crimson clover (10)	Radish (4)

five irrigation events ($88.90\,mm$) during the growth season. The no-tillage technique was applied in 2020 for both crops.

In 2021, corn was planted on April 16 and harvested on September 9, 2021. The corn variety was CP56-78VTP2. 77,854 seeds/ha (31,500 seeds/A), planted at a depth of $3.80\,cm$ with a row spacing at $91\,cm$. Corn received two rounds of fertilizers ($284\,kg/ha$ fertilizer $17-17-17$ and $112.25\,kg/ha$ fertilizer $28-0-0-5$) and one irrigation event ($22.86\,mm$) during the corn season. Soybeans were planted on June 16 and were harvested on November 7, 2021. The soybean variety was AG69XFO. 290,000 seeds/ha (8.8 seeds/ft), planted at a depth of $1.90\,cm$ and spacing at $91\,cm$. For soybean 2021, no fertilizers were applied, and just one irrigation ($22.86\,mm$) event was applied. Strip-till technique was applied for both crops in 2021. Crops were harvested in both years with an Almaco R1 combine machine (Almaco, Danfoss Group, Neveda, IA, USA, 2022).

Soil Hydrology Assessment 2020

In 2020, the infiltration was measured once per season in each plot using the Saturo (Figure 2.6) (Meter Group, Pullman, WA, USA) and the infiltrometer SMS (Soil Measurement Systems, Tucson, AZ, USA, 1987). There was just one reading per plot in each season with the Saturo. One

reading during spring (March 2020) with cover crops and one reading during summer (August 2020) with the cash crops (Figure **??** and **??**). The Saturo measures the field saturated hydraulic conductivity (K_{fs}). The Saturo uses pressure heads analysis to correct the data obtained from the ring infiltrometer. This automated machine reduces errors in the hydraulic conductivity data measured (Reynolds, Topp, & Vieira, 1992). There are four main components included in the Saturo: the insertion metal ring, the control unit, the infiltrometer head, and a water supply tank.

Figure 2.4: Saturo measurements in the radish, cereal rye, and crimson clover cover crop plots during spring.

Figure 2.5: Saturo measurements in the cash crop plots (corn and soybean) during summer.

In each plot, one meter of margin was taken as protection, and the Saturo was installed in the row of the crops inside of the area protected by the margin. In the area where the Saturo was installed, rocks, sticks, and vegetation were removed from the surface. The vegetation was clipped

Figure 2.6: Saturo and its components, metal ring, pressure chamber, water supply tank, and the control unit.

close to the surface of the soil, leaving the root system and removing the green biomass part of the plants. The insertion ring was installed flush with the top of the soil ($5\,cm$ depth), ensuring there were no gaps between the soil and the ring sidewalls. The infiltrometer head was clamped onto the insertion ring to form a seal. Hoses, sensor cables, and water supply were connected to the designated head and the control unit. Test settings were configured, and the test started running. Test settings are shown in Table 2.2.

Table 2.2: Test sittings of the Saturo in the control unit during the infiltration measurement.

Pressure Head 1 (cm)	5.0
Pressure Head 2 (cm)	10.0
Soak Time (min)	20
Pressure Cycles	3
Hold Time (min)	15
Insertion Depth (cm)	5
Run Time (min)	110

It was necessary for a hydrostatic pressure between 5 and $10\,cm$ for the pressure heads. Pressure heads varied depending on the type of soil. The ring was inserted at $5\,cm$ depth. A low-pressure head was applied in soils with high infiltration rate and a high-pressure head in soils with

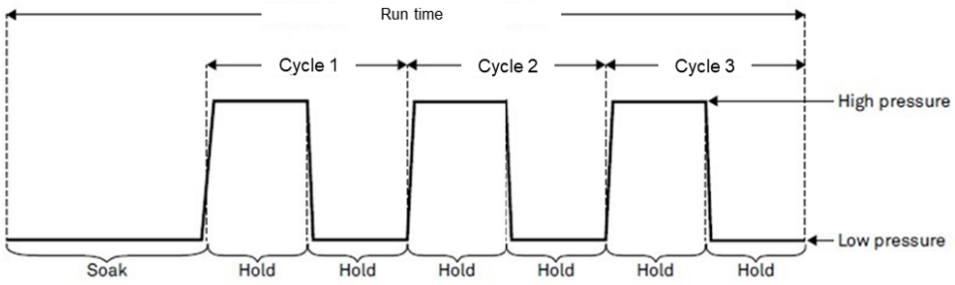

Figure 2.7: Saturo run time diagram of 110 minutes, soak time and three cycles of high and low pressure.

low infiltration rate. A difference of $5\,cm$ between the low and high-pressure heads was applied. The chamber of the Saturo applied water before the pressure cycles began to saturate the soil. The Saturo took 15 to 20 minutes to soak the soil at the beginning of each measurement. This soaking time depended on the soil characteristic type. The pressure head was low during the soak time. Two pressure heads runnings (high - low pressures) were equal to one pressure cycle (110 minutes) (Figure 2.7). The field saturated hydraulic conductivity (K_{fs}) was estimated in the last cycle through the median infiltration rate of the different pressure heads. The steady-state infiltration was obtained by several pressure cycles of the Saturo (Figure 2.7).

For evaluating the infiltration and unsaturated hydraulic conductivity, an SMS tension infiltrometer was used (Figure 2.8). The SMS infiltrometer includes; the water reservoir, which empties as water flows into the soil, the $1.27\,cm$ (1/2") ID tube between the disk, the water tower, the bubble tower which controls tension at the soil surface, and the disk to establish hydraulic continuity with the soil. The surface was cleaned in a $40\,cm$ diameter, and the metal ring was gently pressed into the soil. Fine sand was used as the contact material, placed in the ring, and leveled with a straightedge.

The infiltrometer disk was centered on the ring and pressed down onto the contact material. The connection between the contact material/disk was inspected to assure good conductivity. Incorrect contact between the sand/disk results in only partial flow across the disk diameter and poor infiltration data (Reynolds & Elrick, 1991). Two tension measurements were taken. The high tension of $15\,cm$ and the low tension of $6\,cm$. First, $15\,cm$ tensions were taken together with the time

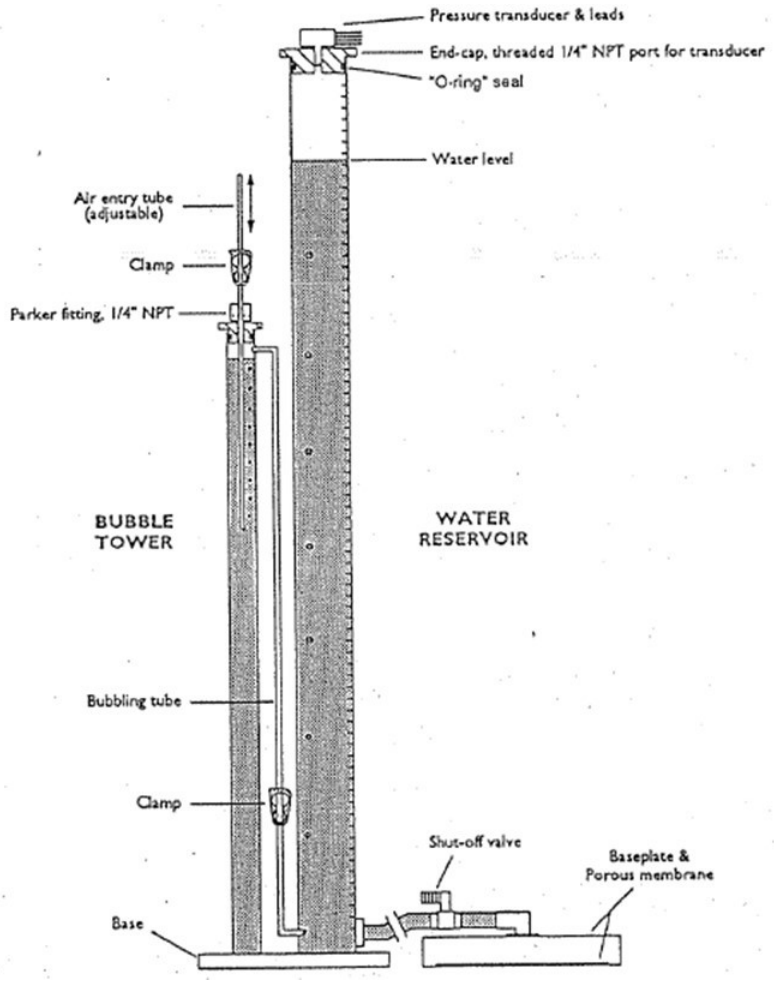

Figure 2.8: SMS Tension Infiltrometer, the bubble tension tower, water tank tower, and the disk. (Soil Measurement Systems., Tucson, AZ, USA, 1987).

until a steady-state infiltration rate was reached. Then, the tension was decreased to $6\,cm$. For the tension of $6\,cm$, the water level was read every centimeter. The time for the steady-state infiltration rate depends on the water content and the hydraulic properties of each soil (White, Sully, & Perroux, 1992). In general, dry soils have higher hydraulic conductivities and faster infiltration. Wet soils take more time to reach steady-state infiltration rates. The hydraulic conductivity can be calculated by (Wooding, 1968):

$$Q = \pi r^2 K \left[1 + \frac{4}{\pi r \alpha}\right] \tag{2.1}$$

This equation was presented by Wooding to calculate the steady-state infiltration rates using a circular source radius r (cm). Q is the water volume entering into the soil per unit time ($cm^3\,hr^{-1}$), K ($cm\,hr^{-1}$) is the hydraulic conductivity, and α ($cm\,hr^{-1}$) is an emperical fitting parameter. It is known that the unsaturated hydraulic conductivity of soil changes with the matric potential h (cm) as presented by Gardner (1958):

$$K(h) = K_{sat} exp(\alpha h) \tag{2.2}$$

Where K_{sat} is the saturated hydraulic conductivity ($cm\,h^{-1}$) and h (cm) is the matric potential or tension at the source. While equation 2.1 is applied for unsaturated and ponded infiltration, equation 2.2 is used only for $h \leq 0$ to measure the volume of water (Q) with the tension infiltrometer per unit time through the porous membrane at a minimum of two tensions. For unsaturated soil, replacing K in equation 2.1 with K_{sat} exp (αh), and the replacement of equations h_1 and h_2, respectively for h in the combined equation 2.1 obtains:

$$K(h_1) = \pi r^2 K_{sat} exp(\alpha h_1) \left[1 + \frac{4}{\pi r \alpha}\right] \tag{2.3}$$

$$K(h_2) = \pi r^2 K_{sat} exp(\alpha h_2) \left[1 + \frac{4}{\pi r \alpha}\right] \tag{2.4}$$

dividing equation 2.4 by equation 2.3 and solving for α yields:

$$\alpha = \frac{ln\Big[Q(h_2)/Q(h_1)\Big]}{h_2 - h_1} \tag{2.5}$$

Alpha (α) can be calculated directly from equation 2.5 because $Q(h_1)$, $Q(h_2)$, h_1, and h_2 are measured and known.

Soil Hydrology Assessment 2021

Soil hydrological properties were measured in 2021 differently than in 2020. In 2020, it was noticed that the hydraulic conductivity data was being affected by the row of the crops. For 2021, it was decided to collect the hydraulic conductivity data in the row of the crops but also on the side of the cover crop row (right and left sides) to obtain better infiltration data. In 2021, a ring infiltrometer was used to obtain the infiltration rate. The infiltration rate and soil samples were taken at five points per plot, one in the row of the crop and two more readings on each side of the crops (Figure 2.9) The area selected for the ring infiltrometer was cleaned. The vegetation on the surface was cut and removed while the root system of the plants remained *in situ*. Per each plot, a soil sample was taken to analyze for particle size distribution and to calculate the initial gravimetric water content. A second soil sample was collected to determine the bulk density. Finally, the metal ring was inserted into the soil at a depth of $1\,cm$.

Soil hydrology was evaluated in 2021 through the BEST-1K method. BEST-1K estimates hydraulic parameters based on the particle-size analysis and infiltration observations (Lassabatère et al., 2006).

A depth of $1.2\,cm$ of water was discharged into the metal ring infiltrometer at time zero, and the time passed by during the infiltration of the known volume of water was read. After the first water volume was completely infiltrated, another volume of $1.2\,cm$ of water was diverted to the ring infiltrometer, and the time needed for it to infiltrate was read (cumulative time) (Figure 2.10). After infiltration, the water content was taken in all five locations A, B, C, D, and E (Figure 2.9).

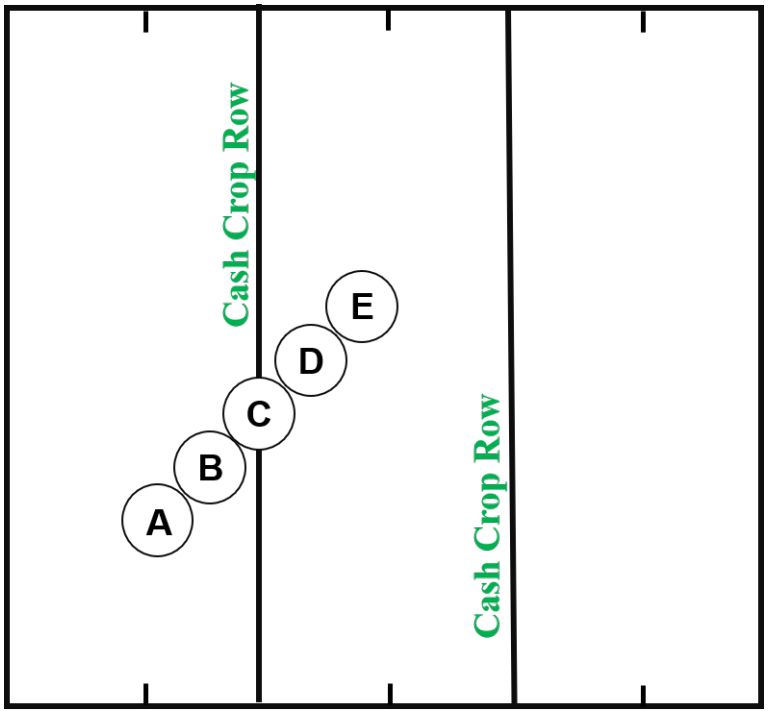

Figure 2.9: Locations A, B, C, D, and E, where data and soil samples were taken for the BEST method.

However, bulk density and particle soil distribution (PSD) parameters were taken in all locations except at location C. It was not possible to extract an undisturbed sample due to the cash crop rooting system. This method was repeated for a run of about 8 to 12 known water volumes, and cumulative infiltration was recorded. Afterward, a saturated soil sample was taken to obtain the water content and the initial water content from the bulk density, contemplating the water density as $1\ g/cm^3$ (Lassabatère et al., 2006).

2.3.3 Statistical Analysis

Cover crop treatments and season effects were determined from the analysis of variance (ANOVA) for main and interaction effects during 2020. One-way ANOVA was performed to assess cash crop (crop) and cover crop (treatment) effects on the estimated soil hydrology parameters hydraulic conductivity and sorptivity (an avarage of the readings per plot) for each BEST method during 2021. ANOVA was performed in R (R Core Team, 2022). Afterward, a posthoc analysis was

Figure 2.10: Ring infiltrometer in one of the points where data was collected during 2021 for the BEST-1K.

performed with a Fisher-LSD test and a Bonferroni correction at a significant level of $\alpha = 0.05$-level using the R package agricolae for each crop and methodology (De Mendiburu, 2021). Results were grouped according to their level of significance. Each group is identified by a letter in the Figures and Tables.

2.4 Results and Discussion

2.4.1 Saturo

Significant differences in hydraulic conductivity were found between treatments ($P < 0.025$) and season ($P < 0.013$) for soybeans in 2020 (Table 2.3). During spring, crimson clover (a) obtained the highest hydraulic conductivity numerically with $8.34\,cm/h^{-1}$ but not different from cereal rye ($4.30\,cm/h^{-1}$) and radish ($6.54\,cm/h^{-1}$), having a similar result (ab). However, fallow (b) got the lowest hydraulic conductivity numerically in spring with $1.43\,cm/h^{-1}$. During the summer, crimson clover (a) obtained the highest hydraulic conductivity numerically ($11.30\,cm/h^{-1}$) as in spring,

Table 2.3: Saturo and tension infiltrometer summary of the analysis of variance (ANOVA) for the linear model applied for the saturated hydraulic conductivity, treatment and season for soybean and corn during 2020. Post hoc analysis was applied for each crop specie.

Season	**Treatment**	**Saturo**		**Tension Infiltrometer**	
		Soybean	**Corn**	**Soybean**	**Corn**
Spring		**cm/h**	**cm/h**	**cm/h**	**cm/h**
	Fallow	1.43 b	1.55 a	23.14 c	10.84 b
	Cereal Rye	4.30 ab	4.65 a	28.10 c	34.80 ab
	Crimson Clover	8.34 a	6.73 a	33.26 bc	9.98 b
	Radish	6.54 ab	3.40 a	28.46 c	31.03 ab
Summer	Fallow	9.25 a	10.20 a	380.75 ab	327.68 a
	Cereal Rye	4.35 ab	4.36 a	503.63 a	193.65 a
	Crimson Clover	11.30 a	6.51 a	946.06 a	74.70 ab
	Radish	10.40 a	7.49 a	441.50 a	222.58 a
		P>F	**P>F**	**P>F**	**P>F**
Season (S)		0.013	0.039	<0.001	<0.001
Treatment (T)		0.025	0.661	0.232	0.110
S x T		0.632	0.093	0.711	0.689

but fallow (a) increased the hydraulic conductivity 6.46 times more than in spring. However, there was no significant hydraulic conductivity difference between radish (a) ($10.40\,cm/h^{-1}$), crimson clover, and fallow ($9.25\,cm/h^{-1}$) treatments, but cereal rye (ab) maintained the same hydraulic conductivity level as in spring ($4.35\,cm/h^{-1}$) (Table 2.3). There was no statistical interaction between the treatments and the seasons for soybeans.

There was a significant difference between seasons ($P < 0.039$) but not between treatments ($P > 0.661$) during 2020 for corn measured by Saturo (Table 2.3). During spring, there was no difference between treatments (a). However, crimson clover obtained the highest hydraulic conductivity numerically ($6.73\,cm/h^{-1}$), followed by cereal rye ($4.65\,cm/h^{-1}$), radish ($3.40\,cm/h^{-1}$), and finally fallow with the lowest hydraulic conductivity numerically ($1.55\,cm/h^{-1}$). During summer, there was no hydraulic conductivity difference between the treatments (a). However, the hydraulic conductivity increased in the fallow plot 6.5 times during the summer ($10.20\,cm/h^{-1}$) in comparison to spring. The hydraulic conductivity in radish increased twice during the summer ($7.49\,cm/h^{-1}$) in comparison to spring, but cereal rye ($4.36\,cm/h^{-1}$) and crimson clover

($6.51\,cm/h^{-1}$) maintained similar hydraulic conductivity in summer in comparison to spring. Interaction between the treatments and the season for corn was not significant.

Comparing the hydraulic conductivity between cash species, fallow and cereal rye treatments had similar hydraulic conductivity in each crop during the same seasons. On the other hand, the hydraulic conductivity in crimson clover and radish treatments for soybean was higher in both seasons compared with corn.

2.4.2 Tension Infiltrometer

There was a significant hydraulic conductivity difference between seasons ($P < 0.001$) for soybeans (Table 2.3). During spring, crimson clover (bc) had the highest hydraulic conductivity numerically ($33.26\,cm/h^{-1}$), followed by radish ($28.46\,cm/h^{-1}$) and cereal rye ($28.10\,cm/h^{-1}$) both with similar hydraulic conductivity (c). Finally, fallow (c) had the lowest hydraulic conductivity numerically in spring ($23.14\,cm/h^{-1}$). During summer, there was a significant hydraulic conductivity difference between the treatment as well. However, crimson clover (a) obtained the highest hydraulic conductivity numerically ($946.06\,cm/h^{-1}$) like in spring, followed by cereal rye (a) ($503.63\,cm/h^{-1}$), radish (a) ($441.50\,cm/h^{-1}$), and fallow (ab) plot ($380.75\,cm/h^{-1}$). There was no significant hydraulic conductivity difference between treatments ($P > 0.232$) during spring and summer. There was no interaction between treatments and seasons ($P > 0.711$).

For corn, it was found a significant hydraulic conductivity difference between seasons ($P < 0.001$) (Table 2.3). In spring, Cereal rye obtained the higest hydraulic conductivity numerically ($34.80\,cm/h^{-1}$), followed by radish ($31.03\,cm/h^{-1}$) with similar result (ab), fallow ($10.84\,cm/h^{-1}$), and crimson clover ($9.98\,cm/h^{-1}$) with similar results as fallow (b). During summer, fallow obtained the highest hydraulic conductivity numerically ($327.68\,cm/h^{-1}$), followed by radish ($222.58\,cm/h^{-1}$), cereal rye ($193.65\,cm/h^{-1}$), and crimson clover (ab) with the lowest hydraulic conductivity numerically ($74.70\,cm/h^{-1}$). There was no significant difference between treatments ($P > 0.110$). Moreover, there was no significant interaction between the treatments and seasons ($P > 0.689$).

2.4.3 BEST-1K

The BEST-1K algorithm estimates the soil hydraulic parameters for the Best-Slope (Lassabatère et al., 2006), Best-Intercept (Yilmaz, Lassabatere, Angulo-Jaramillo, Deneele, & Legret, 2010), and Best-steady methods (Bagarello, Di Prima, & Iovino, 2014). In this study, we present the results from the Best-Intercept and the BEST-Steady method because the BEST-Slope method resulted in negative estimates for the hydraulic conductivity.

Hydraulic Conductivity estimated by BEST-Intercept and BEST-Steady

There was no significant hydraulic conductivity difference between treatments ($P > 0.158$) for corn by the BEST-Intercept (Table 2.4). However, cereal rye (a) obtained the highest hydraulic conductivity numerically ($5.15\,cm/h^{-1}$), followed by radish (a) ($3.54\,cm/h^{-1}$), fallow (a) ($3.42\,cm/h^{-1}$), and crimson clover (a) ($3.28\,cm/h^{-1}$). For soybeans, there was no significant hydraulic conductivity difference between treatments ($P > 0.588$) by the BEST-Intercept as well (Table 2.4). However, cereal rye (a) obtained the highest hydraulic conductivity numerically ($1.99\,cm/h^{-1}$) followed by fallow (a) plot ($1.81\,cm/h^{-1}$), radish (a) ($1.66\,cm/h^{-1}$), and crimson clover (a) ($1.35\,cm/h^{-1}$). The hydraulic conductivity in the corn plots was higher compared with soybean plots by the BEST-Intercept method. On average, the hydraulic conductivity increased from $1.35\,cm\,h^{-1}$ (soybeans) to $3.42\,cm\,h^{-1}$ (corn). There were no significant effects of cover crops on hydraulic conductivity for both crops (Table 2.4).

The results for the hydraulic conductivity estimated by the BEST-Steady method had the same tendency as the estimates from the BEST-Intercept method. There was no significant hydraulic conductivity between treatments ($P > 0.513$) for corn by the BEST-Steady (Table 2.4). Cereal rye (a) obtained the highest hydraulic conductivity numerically ($2.61\,cm/h^{-1}$), followed by radish (a) ($2.02\,cm/h^{-1}$), fallow (a) ($2.02\,cm/h^{-1}$), and crimson clover (a) ($1.95\,cm/h^{-1}$). For soybeans, there was no significant hydraulic conductivity difference between treatments ($P > 0.220$) by the BEST-Steady method (Table 2.4). Cereal rye (a) obtained the highest hydraulic conductivity numerically ($1.60\,cm/h^{-1}$) followed by fallow (a) plot ($1.29\,cm/h^{-1}$), radish (a) ($1.01\,cm/h^{-1}$),

and crimson clover (a) ($0.92\,cm/h^{-1}$). On average the hydraulic conductivity increased from $0.92\,cm\,h^{-1}$ (soybeans) to $1.95\,cm\,h^{-1}$ (corn) comparing both crop by the BEST-Steady methodology. There were no significant effects of cover crops on hydraulic conductivity (Table 2.4).

Table 2.4: Summary of the analysis of variance of the hydraulic conductivity estimated by the BEST-Intercept and the BEST-Steady methods for corn and soybean during 2021. Post hoc analysis was applied for each crop species and methodology.

Parameter	**Treatment**	**BEST- Intercept**		**BEST-Steady**	
		Corn	**Soybean**	**Corn**	**Soybean**
		cm/h $^{-1}$	**cm/h $^{-1}$**	**cm/h $^{-1}$**	**cm/h $^{-1}$**
Hydraulic conductivity	Fallow	3.42 a	1.81 a	2.02 a	1.29 a
	Cereal Rye	5.15 a	1.99 a	2.61 a	1.60 a
	Crimson Clover	3.28 a	1.35 a	1.95 a	0.92 a
	Radish	3.54 a	1.66 a	2.02 a	1.01 a
		P>F	**P>F**	**P>F**	**P>F**
Treatments		0.158	0.588	0.513	0.220

Sorptivity estimated by BEST-Intercept and BEST-Steady

Table 2.5: Summary of the analysis of variance of the sorptivity estimated by the BEST-Intercept and the BEST-Steady methods for corn and soybean during 2021. Post hoc analysis was applied for each crop species and methodology.

Parameter	**Treatment**	**BEST- Intercept**		**BEST-Steady**	
		Corn	**Soybean**	**Corn**	**Soybean**
		cm/h $^{-0.5}$	**cm/h $^{-0.5}$**	**cm/h $^{-0.5}$**	**cm/h $^{-0.5}$**
Sorptivity	Fallow	6.21 a	2.86 a	4.73 a	2.53 a
	Cereal Rye	8.20 a	3.42 a	5.87 a	3.05 a
	Crimson Clover	6.35 a	2.97 a	4.92 a	2.49 a
	Radish	6.75 a	4.45 a	5.12 a	3.48 a
		P>F	**P>F**	**P>F**	**P>F**
Treatments		0.080	0.116	0.228	0.246

There was no significant sorptivity difference between treatments ($P > 0.080$) for corn estimated by BEST-Intercept (Table 2.5). Cereal rye (a) obtained the highest sorptivity numerically ($8.20\,cm\,h^{-0.5}$), followed by radish (a) ($6.75\,cm\,h^{-0.5}$), crimson clover (a) ($6.35\,cm\,h^{-0.5}$), and fallow (a) ($6.21\,cm\,h^{-0.5}$). For soybeans (Table 2.5), there was no significant sorptivity difference between the treatments ($P > 0.116$) as well estimated by BEST-Intercept. However, radish obtained

the highest sorptivity numerically (a) ($4.45\,cm\,h^{-0.5}$), followed by cereal rye (a) ($3.42\,cm\,h^{-0.5}$), crimson clover (a) ($2.97\,cm\,h^{-0.5}$), and fallow (a) plot ($2.86\,cm\,h^{-0.5}$). The sorptivity in the corn plots was significantly higher compared with soybean plots by the BEST-Intercept (Table 2.5). On average, the sorpitivity increased from $2.97\,cm\,h^{-0.5}$ (soybeans) to $6.35\,cm\,h^{-0.5}$ (corn). There were no significant effects of cover crops on sorptivity by the Best-Intercept (Table 2.5).

The sorptivity in the corn plots was almost 50% higher compared with soybean plots estimated by BEST-Steady as in BEST-Intercept. In corn, cereal rye (a) obtained the highest sorptivity numerically ($5.87\,cm\,h^{-0.5}$), followed by radish (a) ($5.12\,cm\,h^{-0.5}$), crimson clover (a) ($4.92\,cm\,h^{-0.5}$), and fallow (a) ($4.73\,cm\,h^{-0.5}$). For soybeans, there was no significant sorptivity difference between the treatments ($P > 0.246$) as in corn ($P > 0.228$) by the BEST-Steady. Radish obtained the highest sorptivity numerically (a) ($3.48\,cm\,h^{-0.5}$), followed by cereal rye (a) ($3.05\,cm\,h^{-0.5}$), fallow (a) plot ($2.53\,cm\,h^{-0.5}$), and crimson clover (a) ($2.49\,cm\,h^{-0.5}$). On average, the sorptivity increased from $2.49\,cm\,h^{-0.5}$ (soybeans) to $4.92\,cm\,h^{-0.5}$ (corn). There were no significant effects of cover crops on sorptivity (Table 2.5).

2.4.4 Crop Yield

Corn Yield

There was no significant yield difference between treatments ($P > 0.776$) for corn during 2020. However, plot number six with two cover plant mixes (cereal rye-crimson clover) obtained the highest corn yield numerically ($15.25\,t/ha$). The lowest corn yield numerically ($10.88\,t/ha$) was obtained in the plot number 11 with a mix of three plant species (cereal rye-crimson clover-radish) (Table 2.6). In 2021, it was found no significant yield difference between the treatment ($P > 0.398$) for corn as well. The yield obtained in the plots treatments were similar to each other (a). However, the treatment with cereal rye got the highest corn yield numerically ($11.30\,t/ha$). The lowest numerically corn yield was found in the clover-radish treatment ($6.01\,t/ha$). Other treatments obtained corn yield between these two ranges (Table 2.6).

Table 2.6: Summary of the analysis of variance (ANOVA) for corn yield during 2020 and 2021 and the cover crops. Numbers in the parenthesis is the seed planting range (kg/ha). The post hoc analysis was applied for each treatment and year.

Trt	Species	2020	2021
		kg/ha	**Kg/ha**
1	Fallow (80)	13.22 a	8.30 a
2	Rye (90)	13.68 a	11.30 a
3	Clover (20)	12.74 a	10.55 a
4	Radish (8)	15.04 a	8.77 a
5	Rye-Clover (65)	13.90 a	10.81 a
6	Rye-Clover (50)	15.25 a	9.07 a
7	Rye-Radish (53)	13.38 a	10.80 a
8	Rye-Radish (38)	12.62 a	8.18 a
9	Clover-Radish (28)	11.54 a	10.43 a
10	Clover-Radish (18)	11.36 a	6.01 a
11	Rye-Clover-Radish (59)	10.88 a	10.84 a
12	Rye-Clover-Radish (44)	11.16 a	11.00 a
		P>F	**P>F**
	Treatments	0.776	0.398

Soybean Yield

There was a significant yield difference between treatments ($P < 0.030$) for soybeans during 2020. Treatment number ten, with a mix of two plant species (crimson clover-radish), obtained the highest soybean yield numerically (a) with $3.29\,t/ha$. The lowest numerically soybean yield was found in the fallow treatment (b) with $2.75\,t/ha$. Other yield treatments (ab) were between the range of the clover-radish treatment (a) and the fallow treatment (b) (Table 2.7). However, there was no significant yield difference between treatments ($P > 0.862$) for soybeans during 2021. The yield obtained in the plot treatments was similar (a). The highest numerically soybean yield was obtained in the rye-clover-radish treatment ($6.92\,t/ha$). The lowest numerically yield was found in radish treatment ($5.05\,t/ha$) (Table 2.7).

Table 2.7: Summary of the analysis of variance (ANOVA) for the soybean yield and the treatments during 2020 and 2021. Numbers in the parenthesis is the seed planting range (kg/ha).The post hoc analysis was applied for each treatment and year.

Trt	Species	2020		2021	
		kg/ha		Kg/ha	
1	Fallow (80)	2.75	b	6.75	a
2	Rye (90)	3.04	ab	5.66	a
3	Clover (20)	3.14	ab	6.74	a
4	Radish (8)	2.87	ab	5.05	a
5	Rye-Clover (65)	3.19	ab	6.25	a
6	Rye-Clover (50)	3.23	ab	5.97	a
7	Rye-Radish (53)	3.24	ab	6.83	a
8	Rye-Radish (38)	3.22	ab	6.85	a
9	Clover-Radish (28)	3.24	ab	6.06	a
10	Clover-Radish (18)	3.29	a	6.54	a
11	Rye-Clover-Radish (59)	3.20	ab	6.92	a
12	Rye-Clover-Radish (44)	3.17	ab	6.10	a
		P>F		P>F	
Treatments		0.030		0.862	

2.5 Discussion

2.5.1 Saturo

During spring, crimson clover had a higher hydraulic conductivity (Table 2.3). In summer, crimson clover, radish, and fallow plots had similar hydraulic conductivity in soybean. Crimson clover grows well in any type of well-drained soil and prefers sandy loam. It has a high well drain soil demand to grow in perfect conditions. Clovers' root system helps prevent erosion and builds soil (Burket, Hemphill, & Dick, 1997). It prevents nutrient runoff and allows more precipitation to go into the soil (Snapp et al., 2005). Due to crimson clover being a legume plant, it has several nodules in its root system, increasing porosity, holes, and channels for water infiltration and hydraulic conductivity.

Moreover, there was no hydraulic conductivity difference between the treatments in both seasons for corn. However, during summer, the fallow plot had the highest numerically hydraulic conductivity in corn. In summer, corn plants were larger. Consequently, their rooting system grew

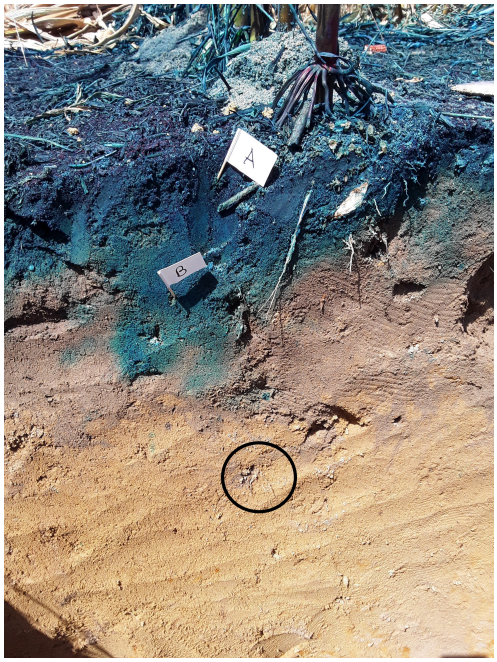

Figure 2.11: Image of the corn root system in a soil profile at the E.V. Smith Research Center at the end of summer 2020. The circle indicates part of the corn root. Deeper corn roots were found in other soil profiles.

and created more pores in the soil and better infiltration in summer than in spring (Ma & Song, 2016). This was confirmed at the end of the summer season in the soil profiles made in the plots treatments. It was seen that corn roots reached long depths (Figure 2.11).

Differences in the hydraulic conductivity in treatments in summer compared with spring are probably attributable to the kind of plant, root system, and plant coverage (Asbjornsen, Shepherd, Helmers, & Mora, 2008). Hydraulic conductivity is influenced by the interactions among root systems, microbiological activities, and soil properties (Bargués Tobella et al., 2014; Benegas et al., 2014; Beven & Germann, 2013). Each plant has an ecological condition and the water demand change from one plant to another. The water demand can vary depending on the growth stage of the crop. Generally, flowering, reproduction, and maturation stages have greater water demand due to the growth of the fruits or the seeds (Asbjornsen et al., 2008). At these different stages, the plant root system grows as well. As a consequence, aggregates, soil structure, and pore space increase resulting from a higher infiltration and hydraulic conductivity.

Blanco-Canqui et al. (2011) found that cover crops resulted in four times greater hydraulic conductivity than when the soil had zero covers. However, the authors explain that these results depend on the season, the growth stage of the different plant species, and the years of applying cover crops in the field. In their study, the infiltration rate increased from one season to another. For instance, soybeans' hydraulic conductivity increases from $2.0\,cm/h^{-1}$ in the initial growth stage of the plant to $3.5\,cm/h^{-1}$ in the late maturing of the species. Similar results were obtained for soybeans in this study in the treatment plots. During spring (initial growth stage of the plant), soybeans increased the hydraulic conductivity from $1.43\,cm/h^{-1}$ to $9.25\,cm/h^{-1}$ in summer (mature growth stage). Authors attributed these results to the plant growth stage and the environmental conditions in each season.

Hubbard et al. (2013) found similar results obtained in this study for corn in the hydraulic conductivity between the cover crops treatments and seasons. The authors measured the hydraulic conductivity three times in different seasons (dates). They found no hydraulic conductivity difference between treatments during the same season. However, the hydraulic conductivity increased from $11.2\,cm/h^{-1}$ in one season to $48.6\,cm/h^{-1}$ in another season. The authors concluded that the difference in the hydraulic conductivity between seasons was due to the environmental conditions and the requirement of each plant species.

Also, results in this study for corn are similar to results obtained by Hubbard, Berdanier, Perkins, and Leonard (1985). The authors found a significant hydraulic conductivity difference between seasons. Hydraulic conductivity increased five times from $6.2\,cm/h^{-1}$ in a season to $31.0\,cm/h^{-1}$ in another season in the same plot. The authors concluded that these results were due to the differences in the root system size from one season to another.

Haruna et al. (2018) studied the infiltration and hydraulic conductivity and found that the hydraulic conductivity was higher in crops in different seasons due to weather conditions and plant growth. The authors evaluated the hydraulic conductivity in cover crops in two different years (2014-2015), and they found that the hydraulic conductivity increased by 66% in all treatments (tillage, no-tillage) from one year to another. For example, the hydraulic conductivity increased by

50% from $3.09\,cm/h^{-1}$ (2014) to $4.56\,cm/h^{-1}$ (2015). The authors suggested that this was due to the higher porosity in soils with crops caused for the roots of the plants. The authors concluded that crops help to break the crusting formed on the surface of soils, helping to increase the infiltration.

2.5.2 Tension Infiltrometer

The ANOVA for the tension infiltrometer (Table 2.3) indicates that the season factor produced a significant effect on the hydraulic conductivity in soybean and corn crops. This means that the season produced important modifications in the conductivity behavior between spring and summer.

Soybean plots obtained the highest hydraulic conductivity during both seasons (Table 2.3). The hydraulic conductivity in soybeans increased from $33.26\,cm/h^{-1}$ in spring to $946.06\,cm/h^{-1}$ in summer. In soybeans, the hydraulic conductivity was three times higher in summer compared to the hydraulic conductivity in corn. The hydraulic conductivity in the fallow plot in both crops was similar in summer. However, a big difference was obtained in the treatments with crimson clover. During summer, in soybeans, the crimson clover got $946.06\,cm/h^{-1}$, and in corn, the hydraulic conductivity was $74.70\,cm/h^{-1}$. This difference is attributed to the weather conditions and the root system size of the plants. During the summer, plants were higher and bigger than in the spring.

The roots and growth stage of plants could influence the difference in hydraulic conductivity between crops during seasons. Roots were probably also responsible for higher hydraulic conductivity in soybeans than in corn. According to Allmaras, Nelson, and Voorhees (1975), "soybean roots have a higher capacity to transmit water flow than corn roots." Soybean roots are thinner than corn roots, and they produce more small pores. It is known that *Leguminosae* plants increase the microporosity reducing the bulk density and increasing absorption of water and minerals by the root system (Singer & Meek, 2004). According to Bouma (1981), there is a rapid downward movement of water (having atmospheric pressure) through micropores in unsaturated soil. Soybean is known for its two typical root systems. The root growing from the hypocotyls in the soybean root system is known as the lateral root. Different root branches are formed from the lateral root of

the soybean root system. The deepest roots may reach down between $0.90\,m$ to $1.45\,m$ or more in loose, well-drained soil (Fenta et al., 2011).

Corn crops produce more big pores due to the kind of root they have. The deepest roots may reach $1.50\,m$. Long roots are a mechanism of the plant to reach the water table, especially in drought seasons (Mengel & Barber, 1974). The deep root system connects with the groundwater and the water table to obtain the water that the plant needs to survive. Roots are very sensitive to the water table. The longer the root, the higher the infiltration and hydraulic conductivity. The hydraulic conductivity with the tension infiltrometer was higher in soybeans due to the smaller pores present in this crop than in corn. Moreover, the hydraulic conductivity was higher in summer than in spring. Different results between seasons were similarly obtained by the Saturo instrument (Table 2.3).

Zumr, Jeřábek, Klípa, Dohnal, and Sněhota (2019) studied the hydraulic conductivity by a tension infiltrometer in grains during different seasons. The authors found that the hydraulic conductivity during the spring was the lowest ($0.06\,cm/h^{-1}$) and then increased during the summer ($0.30\,cm/h^{-1}$). Also, the authors measured the hydraulic conductivity in fall, and the result was the same as in summer. These results were attributed to the root system of the plant and the weather conditions of the seasons.

Those results can be compared to the results obtained by Bhattacharyya, Prakash, Kundu, and Gupta (2006). The authors found a significant difference in the hydraulic conductivity estimated by the tension infiltrometer between grains and legumes. The authors studied the unsaturated hydraulic conductivity in plots established for four years in two different seasons. Legumes (summer) had a higher hydraulic conductivity than grains (spring) in different depths of the soil. At $0 - 75\,mm$ soil depth, legumes obtained an unsaturated hydraulic conductivity $> 100\,cm/h$ than grains that obtained an unsaturated hydraulic conductivity $< 35\,cm/h^{-1}$. The authors concluded that this difference was the result of the presence of more small porosity in the soil in the legumes crop than in the grains crop due to the root systems and weather conditions.

Also, Benjamin (1993) evaluated the hydraulic conductivity using a tension infiltrometer in corn and soybean crops. There were significant hydraulic conductivity differences between crop species ($P < 0.05$) but treatments with the same species. The author measured the hydraulic conductivity in spring and found that soybeans treatments had a higher hydraulic conductivity ($39.9\,cm/h^{-1}$) than corn treatments ($24.6\,cm/h^{-1}$). The author attributed this result to the volume of pore in each crop class.

Differences between the hydraulic conductivity with the tension infiltrometer and the Saturo are due to the way they were measured and calculated. For instance, the hydraulic conductivity in summer in the fallow plot for corn using the Saturo was $10.20\,cm/h^{-1}$ and in the same plot using the tension infiltrometer was $327.68\,cm/h^{-1}$ The hydraulic conductivity was higher with the tension infiltrometer in both seasons and crops than with the Saturo. The data obtained with the tension infiltrometer was processed with equations explained in the methodology (equations 2.1–2.4), and it was found that these formulas overestimated the hydraulic conductivity using the tension infiltrometer for unsaturated hydraulic conductivity. The hydraulic conductivity obtained by Saturo was lower than with the tension infiltrometer even when the hydraulic conductivity was measured and calculated as saturated hydraulic conductivity.

Performance of the BEST-1K Method

The results from these experiments are similar to Haruna et al. (2018). The authors found no hydraulic conductivity and sorptivity statistically differences between treatments in their study. However, treatments with corn obtained the highest numerical hydraulic conductivity ($4.0\,cm/h^{-1}$) and sorptivity ($4.6\,cm\,h^{-0.5}$) than those treatments without any cover vegetation ($2.4\,cm/h^{-1}$ and $0.9\,cm\,h^{-0.5}$). The authors concluded that the sorptivity is affected by the water content of each soil and the kind of crop planted when the infiltration and sorptivity are being studied.

Amer (2020) estimated the sorptivity by the steady method. The author studied the hydraulic conductivity and sorptivity of three soils with different vegetation. The author found that sorptivity was higher in soils with high macroporosity and abundant roots ($3.81\,cm/h^{-1}$) than in those soils

with poor root vegetation ($0.98\,cm/h^{-1}$). The results from Amer (2020) can be confirmed as well as results obtained by the BEST-1K in the corn crops during this research. The author concluded that the high sorptivity is due to higher infiltration and faster capillary flux in soils with macropores and thick roots, especially on the surface. In addition, the author explains that sorptivity and hydraulic conductivity can be higher when the soil is dry than when it is wet.

Thony, Vachaud, Clothier, and Angulo (1991) studied the hydraulic properties of soil and found that in the two areas of study, the sorptivity was influenced by the infiltration time that affected the hydraulic conductivity. In their research, the sorptivity was high and influenced more than 90 percent of the infiltration rate in soils with more porosity ($7.97\,cm/h^{-1}$) due to the size of the pores in the soil caused by different agents than in soils with lower porosity ($1.8\,cm/h$). Similar results were obtained by Smettem and Clothier (1989) studying the sorptivity of soil to estimate the hydraulic conductivity. The authors found that in sandy soils, the sorptivity was higher due to the macroporosity, especially on the surface. The authors (Smettem & Clothier, 1989; Thony et al., 1991) concluded that the sorptivity could be affected by the time to reach the steady-state. Also, they mention that the sorptivity and hydraulic conductivity would be higher on the soil surface, especially in soils with macropores textures or plants that increase this property, such as corn in this study.

Lal and Vandoren (1990) studied the sorptivity and infiltration in plots with 25 years of corn cultivation. They found significant sorptivity differences ($P > 0.05$) between the treatments (moldboard plowing, chisel plowing, and no-till) due to the different agriculture practices applied in each treatment. Probably, there were no significant differences ($P > 0.080$) in this study due to the same agriculture practice applied (these plots were not no-tillage) for all the treatments evaluating the hydraulic conductivity and sorptivity for corn and soybeans. However, the corn treatment with no-tillage obtained the highest sorptivity ($20.2\,cm\,h^{-0.5}$) in their research. The authors attributed this result to the different agriculture practices, plant species, and the time to reach the infiltration rate.

Lassabatère et al. (2006) studied the hydraulic conductivity and sorptivity in three agriculture soils. They found that the BEST-1K was a good method to calculate and obtain the sorptivity and hydraulic conductivity through the measure of infiltration rate by the ring infiltrometer. There were no significant differences between treatments with the sorptivity ($P > 0.05$) but with the hydraulic conductivity ($P < 0.05$). They compared their results with other methods obtaining similar results with the BEST-1K. They concluded that the BEST-1K method is a promising, easy, and cheap method to calculate the hydraulic conductivity.

There were no significant differences between the treatments using the BEST-Steady and the BEST-Intercept. For example, there was no significant hydraulic conductivity difference between the treatments in corn for BEST-Steady and BEST-Intercept. However, the fallow plot for the hydraulic conductivity in corn for BEST-Intercept was $3.42\,cm/h^{-1}$ and for BEST-Steady was $2.02\,cm/h^{-1}$. The BEST-Steady obtained lower data for the hydraulic conductivity and sorptivity than the BEST-Intercept. The data obtained in BEST-Steady was lower because it was more accurate for diagnosing hydraulic conductivity and sorptivity in comparison to the BEST-Intercept. According to Lassabatère et al. (2006), the BEST-Steady is the best way to obtain the hydraulic conductivity and sorptivity using the BEST-1K method.

2.5.3 Crop Yield

Corn Yield

Evaluating the corn yield between treatments, there was no significant productivity difference comparing the fallow plot without cover crops and plots with cover crops during 2020 and 2021 (Table 2.6). A possible reason for this is that corn is a flexible and adapted plant. Soils with the minimum conditions for corn growing can generate a good yield especially when it is irrigated. It is concluded that cover crops did not affect the yield of corn. However, the no difference between treatments could have been to the action of the fertilizers applied during the corn season. With fertilization events in all the plots, corn plants could have gotten the minimum nutrients (Leibig's law of the minimum) required to obtain a favorable production.

Similar results were obtained by several researchers such as Baributsa et al. (2008); Marcillo and Miguez (2017); William and Roth (2017). Marcillo and Miguez (2017) found that the impact of cover crops was neutral to positive in the corn yield through the years. The authors explain that corn yield was not affected by cover crops in some areas for factors such as soil properties, weather conditions, and some types of agriculture technic management. However, corn yield increased by 21 percent in treatments with cover crops after applying for some years; this technique helped reduce the compaction of soil and the bulk density. On the other hand, the authors say that even applying cover crops; the corn yield can be different from year to year due to environmental conditions.

Also, William and Roth (2017) found that there was not a significant corn yield difference between plots with cover crops and without them. The author shows that the impact of cover crops on the corn yield was negligible. Corn yield in treatments was between $11.7\,t/ha$ to $12.1\,t/ha$. The author concluded that cover crops do not influence the corn yield. However, factors such as weed control, soil compaction, planting issues, and environmental conditions often reduce yields.

Baributsa et al. (2008) found that legumes in corn over four years had no impact on corn yields and that the legumes could provide N to a succeeding crop. The authors explain that cover crops did not influence the production of corn plants. However, the author explains that corn yield can vary from year to year due to weather conditions. It can be seen that there were no significant soybean yield differences between treatments as seen with corn. However, soybean yield was higher than corn this year. It is concluded that this difference is not because of the cover crops or soil but weather factors such as temperature and precipitation that affected both crops.

Soybean Yield

ANOVA (Table 2.7) for soybean yield 2020 demonstrated that cover crops increase soybeans productivity. The result was higher in treatments with cover crops than in the fallow treatment. Those results confirmed the results obtained by Capurro (2020). The author found that the soybean yield was 35 percent higher in plots with cover crops ($4.6\,t/ha$) than in plots without cover

crops ($3.4\,t/ha$). However, the author found that corn yield could have a different yield depending on the cover crop species. Plots with cover crops such as vetch and oats did not affect the corn yield ($2.1\,t/ha$) compared with plots without cover crops ($1.5\,t/ha$), but corn yield in plots with Clover ($2.5\,t/ha$) as a cover crop was higher than without any cover crop. The author concluded that yield results could be affected by the cover crop species plants, the years applying cover crops in soil, and weather conditions of the region.

Also, Fernandez, Alvarez, Owen, and Quiroga (2020) observed that soybean yield was higher in plots with cover crops than without them. However, those results were obtained after five years of applying cover crops in the area of study. Soybeans in treatments with cover crops ($4.0\,t/ha$) were higher than those in treatments without cover crops ($1.9\,t/ha$). Those results from Fernandez et al. (2020) can be compared with the results obtained in this research. The authors explain that yield can be increased in crops with cover crops after several years of practicing this agriculture technique and enough presence of water for the crop. Other factors that could contribute to those results were soil type, weather conditions, and fertilization applications.

This information is confirmed by Chalise et al. (2018). The authors explain and point out some of the cover crops' benefits, such as higher yield and infiltrate rate. The authors obtained 14 percent more soybean yield in plots with cover crops compared to plots with no cover crops. The author concluded that cover crops benefit and improve soil hydraulic properties and enhance and increase crop yield.

The ANOVA for soybeans 2021 (Table 2.7) indicated that there was no difference in the soybean yield and treatments during 2021. Calonego, Raphael, Rigon, de Oliveira Neto, and Rosolem (2017) found two times no significant soybean yield difference ($P > 0.05$) between treatments during their study carried on for 12 years. Those results were due to the application of cover crops for two years, which helped to decrease the bulk density and increase the porosity in the soil. The authors explain that these results can vary for weather conditions from year to year and the agriculture technics applied during the study.

Figure 2.12: Soil profiles with high water table at the E.V. Smith Research Center

A similar result was obtained by Acharya, Moorman, Kaspar, Lenssen, and Robertson (2020). The authors found no soybean yield significant differences between treatments with cover crops and treatments with no cover crops twice across three years of studies (2016 ($P > 0.05$), 2017 ($P < 0.05$), and 2018 ($P > 0.05$)). The authors concluded that the difference in the yield depended on the previous agriculture technics applied, seed rate, and weather conditions.

2.5.4 Yield 2020-2021

Comparing the productivity of crops between species, it can be seen in the Tables (2.6 and 2.7) that corn had a higher yield in 2020 than in 2021. The soybean yield almost doubled in 2021 compared to 2020 (Table 2.7). Comparing yield 2020 with yield 2021, corn was harvested less t/ha in 2021 than in 2020. The production of corn decreased in all the plots during 2021 in comparison with the previous year, 2020. By 2021, the growing season was too wet for corn. There was more precipitation in 2021 compared to 2020.

These conditions altered the water table (Figure 2.12), and it could have been a factor that could have affected the corn yields. Corn plants can develop roots deeper than the water table, and this can affect the growing stages of corn plants and the corn yield (Allmaras et al., 1975). It was found that the water table at the E.V. Smith Research Center was few centimeters close to the soil surface in a soil profile made during the study, which means that the water table was high. Nevertheless, the production of 2021 increased for soybean, doubling in some plots. That means that the increment of the soybean yield in 2021 was 100 percent more than the previous year, 2020.

2.6 Conclusions

In the spring before cash crops were planted, the saturated hydraulic conductivity was higher in cover crops than in plots without cover crops. During the summer, the growing cash crop increased the saturated hydraulic conductivity so that there were no detectable differences between cover crops and fallow plots. This is attributed to the sampling location in the cash crop row. To reduce the impact of the cash crop on infiltration data, it is recommended to measure infiltration also outside of the cash crop row. It is also recommended to continue similar experiments on other Alabama benchmark soils.

Corn yield was not affected by the cover crop treatments over the two-year study time. Soybean yield was significantly higher in the cover crop plots in comparison to the fallow plots in 2020. However, there were no differences in 2021. It is assumed that the high water table and the compaction at the field site have compensated for the positive effects of cover crops on hydraulic conductivity and yield reported by other studies. Repeating this trial at a different location in better-drained soil might confirm the positive results reported by other authors.

Chapter 3

Evaluation of the BEST-2K Method to Estimate Soil Hydraulic Parameters

3.1 Abstract

BEST-2K is a method that utilizes saturated and unsaturated infiltration measurements together with the soil particle size distribution to estimate the hydraulic conductivity and soil water retention. Field experiments were conducted at two locations, the Old Rotation and a forest on the Auburn University campus. Estimates from the BEST-2K method were compared to data measured with the HYPROP instrument. The HYPROP is used to measure the water retention curve and the unsaturated hydraulic conductivity of the soil. The BEST-2K method overestimated the volumetric water content of the water retention curve and the hydraulic conductivity for all samples. The root means square error (RSME) of the BEST-2K estimates and the HYPROP data were similar to the RSME of HYPROP field replicates. The BEST-2K method is helpful to estimate soil hydraulic properties when HYPROP instruments are not available.

3.2 Introduction

The movement of water is an essential factor in the hydrologic cycle. There are two movements of water in the soil that can be observed, preferential flow and matrix flow. In saturated soils, the preferential flow indicates the movement of water and solutes through pores in the soil, such as cracks, wormholes, and root channels. Matrix flow refers to the slow movement of water through the soil, sampling all the pore spaces. These two types of flow depend on the soil's physical

characteristics, such as the texture and structure Flows in sandy soil will be faster than in clayey soil. Structured soils affect the different kinds of flows due to the arrangement of soil particles forming different structures. It is known that structured soils have a bimodal pore structure (textural pores from the particles and structural pores from the aggregates) (Durner, 1992). To evaluate the preferential and matrix flow, it is important to measure the pore region of each flow type and to know their soil-water characteristic curve. Bimodal soil models are used to measure both fluxes with some soil physical parameters to estimate hydraulic parameters in the soil. Some soil physical parameters can be measured only by specific laboratory equipment such as HYPROP (Haghverdi, Najarchi, Öztürk, & Durner, 2020). However, in areas without the technology and the purchasing power, others methodologies must be applied. These methods must be easy to apply and inexpensive to measure the Hydraulic conductivity, such as BEST-2K.

Lassabatère et al. (2019) created the BEST-2K method derived from the BEST method to estimate bimodal water retention and hydraulic conductivity. It is based on its principle that consists of the hydraulic characterization of single permeability soils (Lassabatère et al., 2006). BEST-2K is the fusion of water infiltration observations performed at two water pressures: one positive and the other negative. Measurements include; water infiltration when the entire pore network and flux (matrix and fast-flow regions) are activated. The most important inputs for BEST-2K incorporate two water infiltration observations; a metal ring infiltration reading to obtain the cumulative bulk infiltration and a tension infiltrometer to get the cumulative infiltration into the matrix region. Other inputs include the soil particle size distribution (PSD), the water contents for the two tests at the beginning and the end of the tension infiltrometer and metal ring infiltrometer observations, and the bulk density (BD) that is used to obtain from the bulk saturated water content and the water retention curve (Lassabatère et al., 2019).

The rationale of this study was based on obtaining some soil hydrology parameters in an easy and low-cost way. The hydraulic conductivity and the water retention curve are two important parameters in soil and crops management. Due to some countries and institutions don't have enough

monetary resources to get technology for studying soil physical parameters, low-cost methodologies are important to develop and confirm their operation to estimate soil criteria. The objective of the research was to estimate the hydraulic conductivity by the BEST-2K method in Alabama.

3.3 Locations

Parameters were taken in two different locations on the Auburn University Campus in Alabama. The first site was located at the Old Rotation. The Old Rotation is a crop rotation experiment on the Auburn University campus for more than 125 years. It was established in 1896 (latitude 32.5934 and longitude -85.4858), and it consists of 6 cropping systems in 13 plots on $0.40\,ha$ of a Pacolet fine sandy loam (Fine, kaolinitic, thermic Typic Kanhapludults). The Old Rotation is the oldest continuous cotton experiment in the world and the third oldest field crop experiment on the same site in the United States. This rotation also includes rotations with corn, soybeans, and small grains and includes winter cover crops (legumes). Data was taken in the non-irrigated area in plot number five with cotton and winter legume (Figure 3.1).

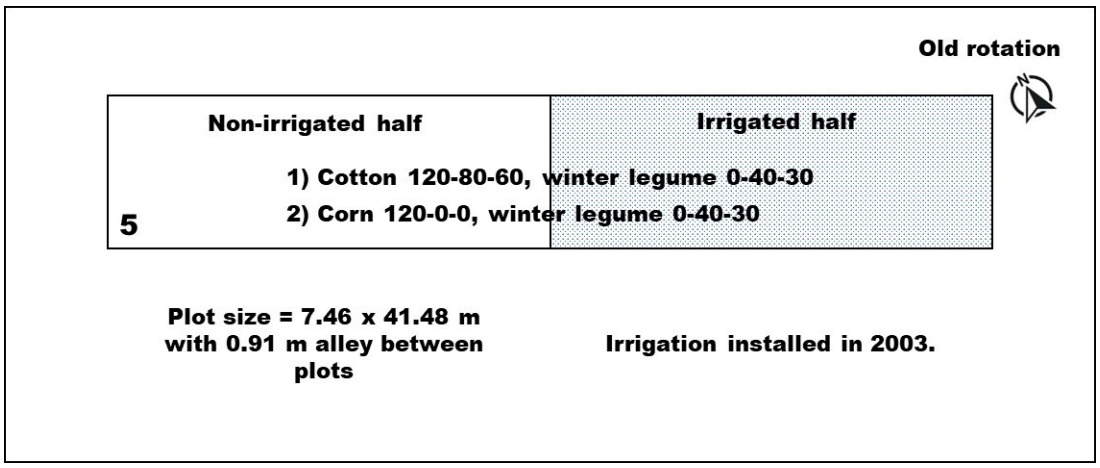

Figure 3.1: Schema of the plot treatments in the Old Rotation with their characteristics (Auburn University, College of Agriculture).

The second site was a forest located behind the Auburn Research and Technology Foundation building on Auburn University Campus (latitude 32.6035 and longitude -85.4917). It has a Marvyn loamy sand (Fine-loamy, kaolinitic, thermic Typic Kanhapludults), and the area is covered

by Loblolly Pine trees (*Pinus taeda*). In those locations, soil samples were taken for laboratory analysis to obtain and calculate unsaturated and saturated hydraulic conductivity, particle size distribution, bulk density, and soil water retention.

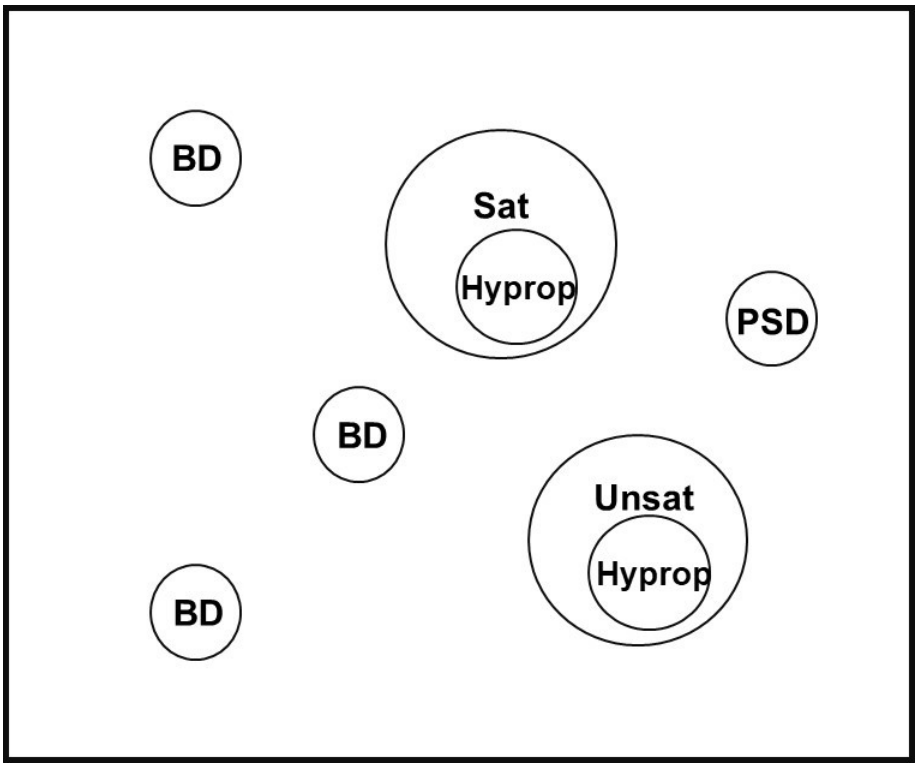

Figure 3.2: BEST-2K schema. Locations: bulk density (BD), particle size distribution (PSD), saturated soil sample (Sat; after saturated infiltration measurement), unsaturated soil sample (Unsat; after tension infiltration measurement), samples taken to be run on the HYPROP instrument (Hyprop).

3.4 Experimental Design

The BEST-2K method estimates the water retention curve (WRC) and the hydraulic conductivity of a dual-porosity soil. It uses the particle soil distribution (PSD) as well as the cumulative infiltration ring and the tension infiltration data. Lassabatère et al. (2019), show the computation in detail. The package Vadoze (Owusu, 2015) was used to fit the PSD parameters (Figure 3.3). On each site of the Old Rotation and Forest, infiltration data was taken with the ring infiltrometer and the tension infiltrometer. Soil samples were taken in each location (Figure 3.2) to measure the

bulk density (ρ_b), particle size distribution, the water content before the infiltration event for the ring infiltrometer ($\theta_{0,B}$), and the tension infiltrometer ($\theta_{0,TI}$) the after infiltration water content for the ring infiltrometer (θ_B), and the tension infiltrometer (θ_{TI}), and the water content for the dual permeability soil ($\theta_{s,2k}$). Lassabatère et al. (2019) used data derived from the BEST-1K. Figure 3.3A, shows a flow illustration at parameters to compute the inputs that would have been obtained with the known metal ring infiltrometer method had each region been sampled separately. The principle of the BEST method (ring infiltrometer) was applied to calculate inputs to determine the hydraulic parameters for each region (Figure 3.3B). The traditional BEST method used in BEST-2K is named BEST-1K for the single permeability, together with BEST-2K for dual-permeability soils. The hydraulic parameters obtained for the matrix and fast-flow regions were used to calculate the hydraulic conductivity and the water retention curve (Figure 3.3C).

Following the methodology by Lassabatère et al. (2019) (Figure 3.3), the precomputing purpose divides the bulk PSD into two distributions, PSD_m and PSD_f, which define the constitution of the matrix and fast flow regions.

$$FF_{2K}(D) = (\tau_f)\Big(1 + (\frac{D_{g,f}}{D})^{Nf}\Big)^{-Mf} + (1 - \tau_f)\Big(1 + (\frac{Dgm}{D})^{Nm}\Big)^{-Mm} \tag{3.1}$$

Where is τ_f the fraction of the fast flow region in the bulk particle size distribution, $FF_{2k}(D)$ the accumulative distribution of particle size, D is the particle diameter θ_f is the fractional contribution of the particles in the fast-flow region, D_g is the mean diameter of particle size mode, and N and M are textural parameters associated by the expression $M = \frac{1-2}{N}$, that is analogous to the Burdine condition. The adjustment for the bulk PSD adds optimized values for N, M, and D_g that calculate the particle size distribution for the matrix and fast-flow regions, PSD_m and PSD_f, respectively. The parameters of the texture (N_m, M_m) and (N_f, M_f), that characterize PSD_m and PSD_f, are inputs to the BEST-1K functions (PTFs), that give the shape parameters of the local water retention fuction in the matrix and fast flow region (n_m, n_f) and the shape parameters of the local hydraulic conductivity fuction in the matrix and fast flow region (η_m, η_f) for the hydraulic conductivity (Lassabatère et al., 2019).

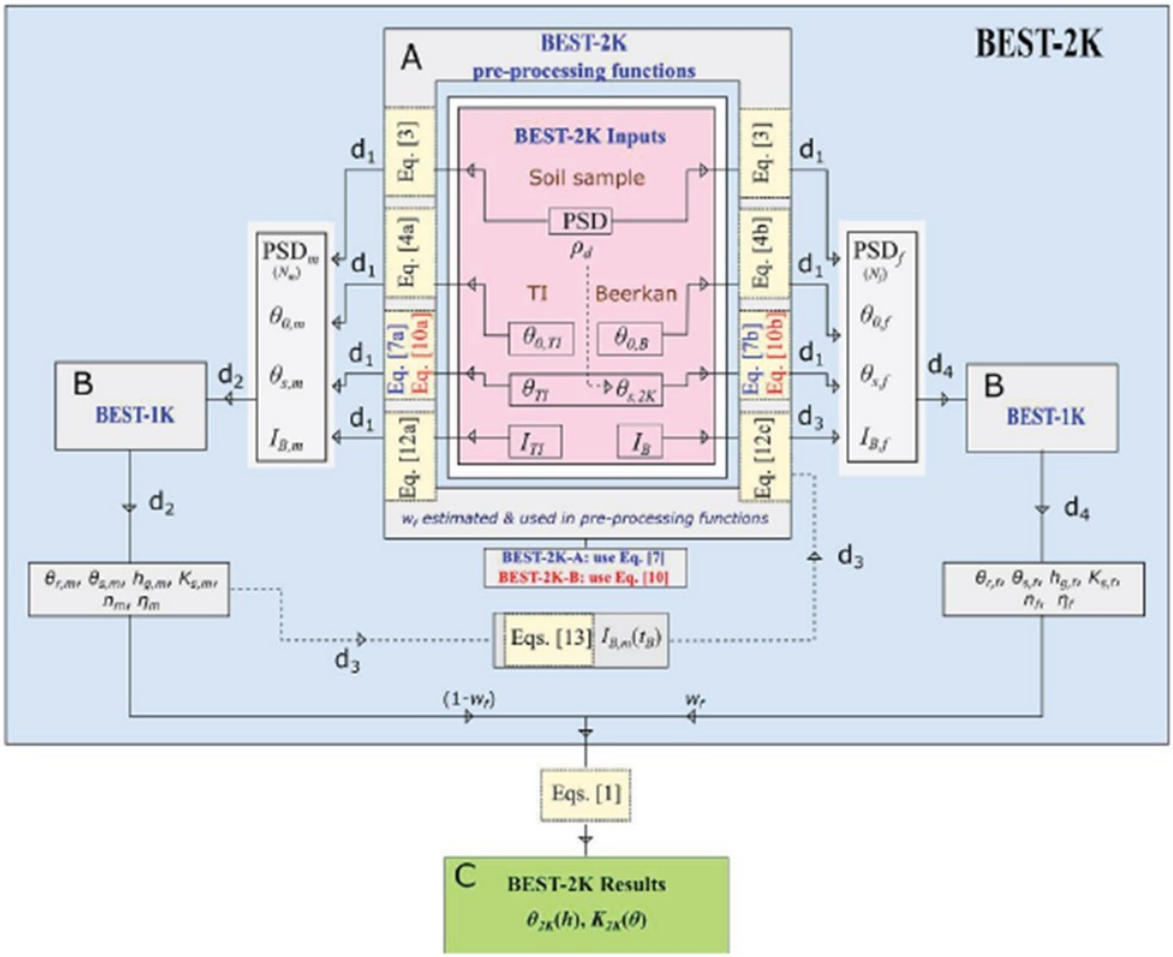

Figure 3.3: BEST-2K methodology diagram by Lassabatere (Lassabatère et al., 2019).

The depth of the infiltration of the tension infiltrometer and the metal ring was calculated in mm. For the tension infiltrometer, the depth was calculated using the radius of the reservoir and the infiltration disk. The depth of the metal ring was calculated by multiplying the increments by the replicates. Then, the single parameters were calculated. The volume fraction of the dual permeability soil occupied by the fast flow region was calculated using the bulk density of the soil, the bulk saturated water content for the dual permeability soil, and the bulk water content at the end of the tension infiltration measurement. Then, the remaining preprocessing parameters were calculated, such as the bulk initial water content for the tension infiltrometer, the local water content in the matrix and the fast flow regions, and finally, the local saturated water content for the matrix and fast-flow region. The PSD was calculated and fit for the particle size distribution of

the fast flow region (PSD_f) and the matrix region (PSD_m) using the PARIO instrument (Meter Group Inc. 2021. USA). The water pressure head of the scale parameters was obtained using the HYPROP. After all the preprocessing parameters were calculated, the BEST-1K was performed for the matrix and the fast flow sections separately. The hydraulic parameters for the dual permeability (DP) soil were calculated, the hydraulic conductivity and the water retention curve were estimated and the root means square error was computed.

3.4.1 Water Retention Curve

The water retention curve and the unsaturated hydraulic conductivity were measured with HYPROP (Meter Group, Pullman, WA, USA). This tool uses two tensiometers in different depths, and it measures the soil water tension and the unsaturated hydraulic conductivity (Figure 3.4). The volumetric water content is obtained from the recording of the weight loss of the sample. With this information, the water retention curve can be represented. First, soil samples were saturated with tap water for 24 hours, closed, and located on a balance. The surface of the soil sample is open to the atmosphere so that way water can evaporate.

The HYPROP reads the water tension in two depths of the soil sample through evaporation using two vertical tension cylinders. The medial pF (suction level) value of the sample is computed based on the average value of the two tensions. The water content is determined based on the weight mass change. The evaporation rate is computed from the weight mass soil differences based on the volume flow at each point in time (Figure 3.5). The hydraulic conductivity values with increasing desiccation correspond to how well the soil can transport this water to the surface, where it evaporates. If the conductivity is low, the soil on the surface dries out, even when the bottom remains wet. The upper tensiometer indicates drier soil than the lower tensiometer, which is still wet. If the conductivity is relatively good, the water in the sample is evaporated, and the other tensiometer shows similar values.

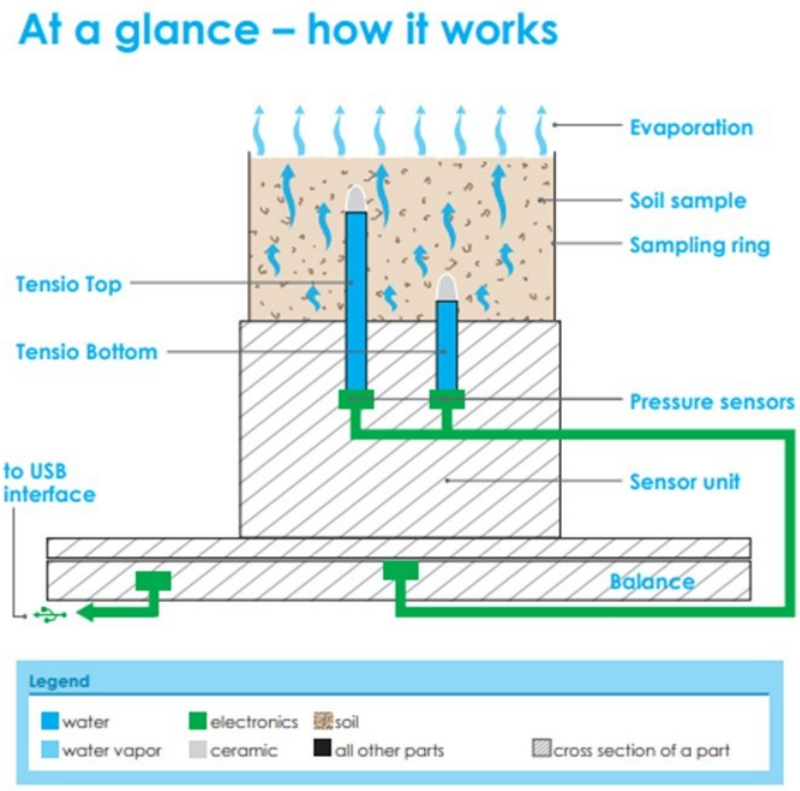

Figure 3.4: HYPROP and its components. Pressure sensors, sensor unit, sampling ring, and balance. (Meter Group Inc. 2021. USA).

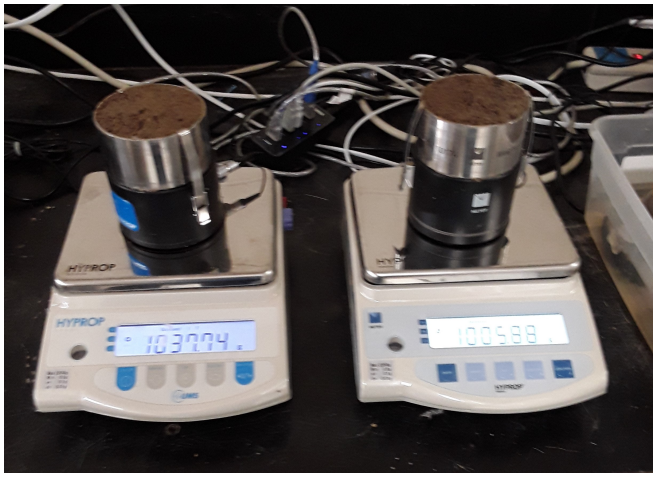

Figure 3.5: Soil samples being read by the HYPROP in the lab.

3.5 Results and Discussion

Soil properties inputs for the BEST-2K were studied and obtained in each location. There is extremely high variability in soil properties between plots in the Old Rotation, nevertheless, results obtained for this study site were similar in the plot. The bulk density was obtained for each study site (Table 3.1). The highest bulk density was found in the Old Rotation one ($1.55\,gr/cm^3$), Followed by the Old Rotation two ($1.41\,gr/cm^3$), Forest one ($1.39\,gr/cm^3$), and Forest two ($1.33\,gr/cm^3$). However, the initial water content before the infiltration experiments with the ring and tension infiltrometer was obtained in Forest one ($0.163\,cm^3\,cm^{-3}$), followed by Old Rotation plot number two ($0.175\,cm^3\,cm^{-3}$), Forest two ($0.201\,cm^3\,cm^{-3}$), and Old Rotation number one ($0.270\,cm^3\,cm^{-3}$). After the infiltration experiments, the water content subsequently in the ring infiltrometer was higher in the Forest sites ($0.397\,cm^3\,cm^{-3}$ and $0.374\,cm^3\,cm^{-3}$), than in the Old Rotation sites ($0.330\,cm^3\,cm^{-3}$ and $0.300\,cm^3\,cm^{-3}$). Notwithstanding, the highest water content after the tension infiltrometer was measured in the Old Rotation number one ($0.349\,cm^3\,cm^{-3}$), followed by the Forest one ($0.339\,cm^3\,cm^{-3}$), Forest two ($0.324\,cm^3\,cm^{-3}$), and finally Old Rotation number two ($0.317\,cm^3\,cm^{-3}$).

Table 3.1: Bulk density, water content before the ring and tension infiltrometer experiments, and the water content after the ring and tension infiltrometer experiments at the Old rotation and Forest sites.

Parameter/Location	**OR.1**	**OR.2**	**FR.1**	**FR.2**
Bulk density (gr/cm^3)	1.55	1.41	1.39	1.33
WC before ring - tension ($cm^3\,cm^{-3}$)	0.270	0.175	0.163	0.201
WC after ring ($cm^3\,cm^{-3}$)	0.330	0.300	0.397	0.374
WC after tension inf. ($cm^3\,cm^{-3}$)	0.349	0.317	0.339	0.324

The particle size distribution was obtained by the Pario instrument in the lab and the soil classification for each soil site (Table 3.2, and Figure 3.6) Alabama soils are known for being very sandy soils and this was confirmed by the results obtained in the lab. Clay particle percentage was similar in the Old Rotation sites ($23.71\,\%$ and $23.31\,\%$). However, clay particle percentage in Forest two was higher ($18.82\,\%$) than in Forest one ($14.68\,\%$). Silt particle percentage was similar

in the Old Rotation sites ($10.97\,\%$ and $10.87\,\%$) but, in the Forest sites silt particles was higher in the Forest one ($12.70\,\%$) compared with Forest two ($3.59\,\%$). The highest sand percent was found in the Forest sites ($77.59\,\%$ and $72.62\,\%$), followed by the Old Rotation sites ($65.70\,\%$ and $65.41\,\%$). Soils in the Old Rotation were classified as sandy clay loam and soils in the Forest sites as sandy loam by the Pario (Table 3.3).

Table 3.2: Particle size distribution obtained of the two study sites in the Old Rotation and the forest by the PARIO (Meter Group Inc. 2021. USA).

Texture Class	**DP[µm]**	**OR.1**	**OR.2**	**FR.1**	**FR.2**
Clay (%)	<2.0µm	23.71	23.31	14.68	18.82
Silt (%)	2.0-50µm	10.87	10.97	12.70	3.59
Sand (%)	50-2000µm	65.41	65.70	72.62	77.59

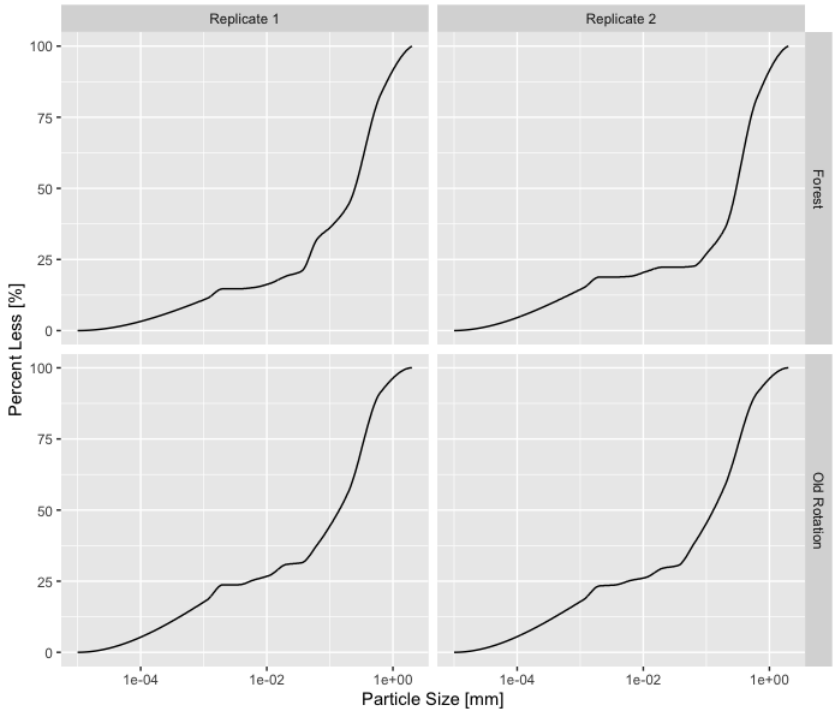

Figure 3.6: Particle size distribution graphic for the two sites in the Old Rotation and Forest site.

Table 3.3: USDA soil texture class obtained by the PARIO (Meter Group Inc. 2021. USA).

Parameter/Location	**Old Rotation**	**Forest**
U.S. Soil taxonomy	Sandy clay loam	Sandy loam

Obtained the most important parameter inputs for the BEST-2K, the fast flow region, hydraulic conductiviy and water retetion curve were calculated. In a dual-porosity water retention model, the parameter w_f indicates the fraction of the soil water retention curve that is affected by the fast-flow region. The w_f values from the HYPROP were similar to the value estimated from BEST-2K for the Old Rotation but were quite different for the Forest (Table 3.4). Results obtained with the HYPROP were higher than the estimated by the BEST-2K due to the HYPROP measured the space ocupaid by the roots of the plants. The BEST-2K methodology is unavailable to estimate this space in the soil sample. For that reason, the fast flow region estimated by the BEST-2K resulted lower in the soil sample of the study area. The fast flow region impacted the hydraulic conductivity, causing a rise in its conductivity level (Table 3.5).

Table 3.4: Fraction for Fast Flow Region (w_f) for the Old Rotation (OR) and forest sites (FR). The numbers indicate field replicates.

HYPROP	OR1	0.362
	OR2	0.386
	FR1	0.752
	FR2	0.567
BEST-2K	OR	0.290
	FR	0.350

The estimated parameters from the BEST-2K method were compared to the water retention and the unsaturated hydraulic conductivity values measured by the HYPROP. To compare the model performance of the BEST-2K method, the root means square error (RMSE) was computed for the measured (HYPROP) and fitted (BEST-2K) data (Table 3.5). The RMSE values for the Old Rotation were lower than for the Forest for both the water retention and the hydraulic conductivity data. For the Old Rotation, the RMSE of the water retention was higher between the two HYPROP field replicates (OR1-OR2, Table 3.5) than between the BEST-2K and the HYPROP measurements. However, for the Forest location, the RMSE between the two field replicates was smaller than the RMSE of the BEST-2K estimates and the HYPROP measurements. For the hydraulic conductivity, the RMSE was lower between the HYPROP field replicates compared to the

RMSE of the BEST-2K and the HYPROP measurements for both locations. The measured and fitted soil water retention curves are illustrated in Figure 3.7 and the hydraulic conductivity is shown in Figure 3.8.

Table 3.5: Root media square error (RMSE) values for the Old Rotation (OR) and forest sites (FR) to compare the BEST-2K method (field replicates indicated with numbers) with the HYPROP (OR1-OR2 and FR1-FR2 values between the field replicates).

		Volumetric water content (cm^3/cm^3)	Hydraulic conductivity (cm/h^{-1})
OR	BEST-2K OR1	0.042	6.194
	BEST-2K OR2	0.029	5.719
	OR1 - OR2	0.044	1.250
FR	BEST-2K FR1	0.077	10.442
	BEST-2K FR2	0.065	7.979
	FR1 - FR2	0.025	1.715

3.5.1 Conclusions and Recommendations

This study applied the BEST-2K method to estimate the hydraulic conductivity in two sites on the Auburn University Campus. The two areas were the Old Rotation site and the forests behind the Auburn Research and Technology Foundation building on Auburn University Campus. For the Old Rotation location, the RMSE for the soil water retention curve was lower between the HYPROP field duplicates in comparison to the BEST-2K estimates and the HYPROP measurements. Although the BEST-2K method has overestimated the soil water content of the water retention curves, the RMSE was still lower than between the field duplicates. This indicates that the spatial variability of the soil water retention curve can be higher than the estimation error of the BEST-2K method. However, field duplicate RMSE was lower for the soil water retention (Forest) and the hydraulic conductivity (Old Rotation and Forest).

Results from this study are limited because of the small number of locations and their close vicinity of them. More research is necessary on different soil types with more field duplicates to unveil when the BEST-2K method produces similar results to the HYPROP instrument. The

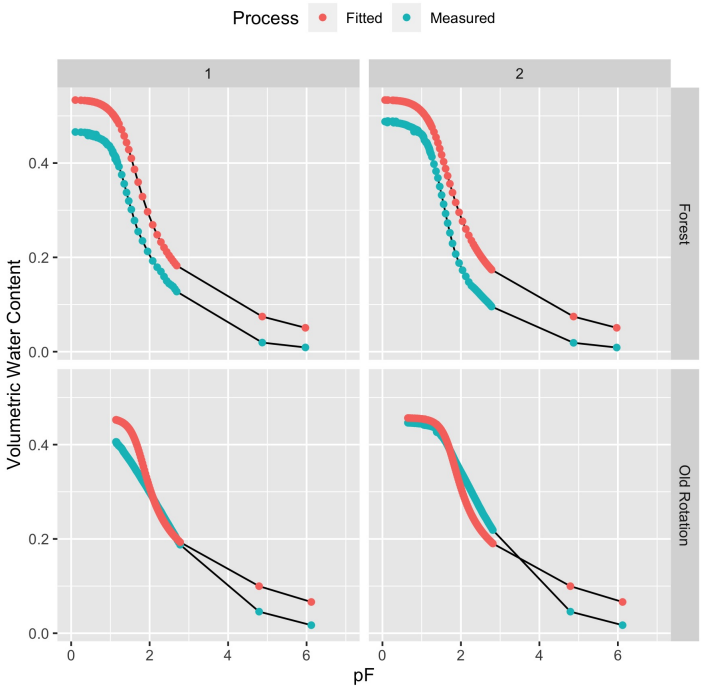

Figure 3.7: Soil water retention curves obtained by the HYPROP (Measured) and estimated by the BEST-2K (Fitted) in the Old Rotation and Forest sites.

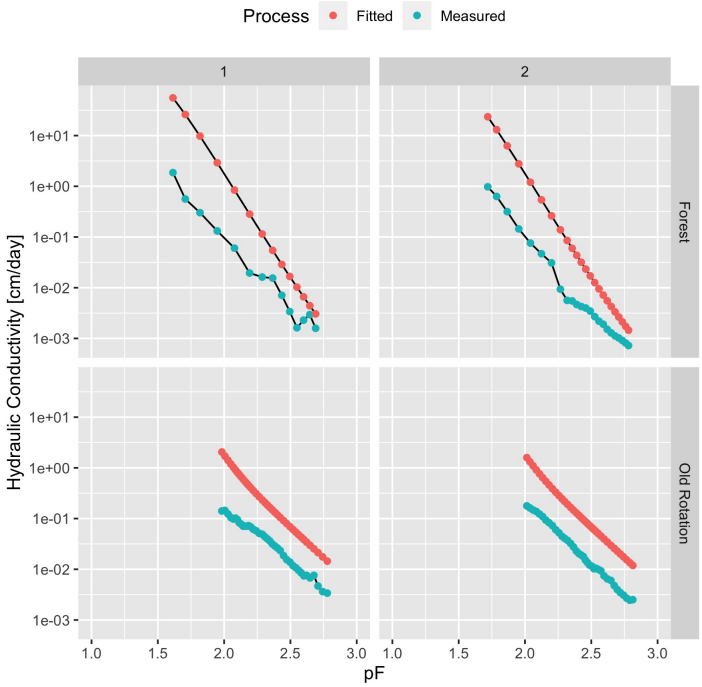

Figure 3.8: The soil hydraulic conductivity obtained by the HYPROP (Measured) and estimated by the BEST-2K (Fitted) in the Old Rotation and Forest sites.

BEST-2K method is useful to estimate soil hydraulic properties when HYPROP instruments are not available.

References

Acharya, J., Moorman, T. B., Kaspar, T. C., Lenssen, A. W., & Robertson, A. E. (2020). Cover crop rotation effects on growth and development, seedling disease, and yield of corn and soybean. Plant Disease, 104(3), 677–687.

Alaoui, A., Caduff, U., Gerke, H. H., & Weingartner, R. (2011). Preferential flow effects on infiltration and runoff in grassland and forest soils. Vadose Zone Journal, 10(1), 367–377.

Allaire, S., Roulier, S., & Cessna, A. (2009). Quantifying preferential flow in soils: A review of different techniques. Journal of Hydrology, 378(1), 179–204.

Allmaras, R., Nelson, W., & Voorhees, W. (1975). Soybean and corn rooting in southwestern minnesota: Ii. root distributions and related water inflow. Soil science society of America Journal, 39(4), 771–777.

Alsherif, N., Wayllace, A., & Lu, N. (2015). Measuring the soil water-retention curve under positive and negative matric suction regimes. Geotechnical Testing Journal, 38, 1–10.

Amer, A. M. A. (2020). Hydraulic conductivity and sorptivity at unsaturated and saturated conditions as related to water infiltration in soils. Eurasian Journal of Soil Sciences, 1–9.

Angulo-Jaramillo, R., Bagarello, V., Di Prima, S., Gosset, A., Iovino, M., & Lassabatere, L. (2019). Beerkan estimation of soil transfer parameters (best) across soils and scales. Journal of Hydrology, 576, 239-261.

Asbjornsen, H., Shepherd, G., Helmers, M., & Mora, G. (2008). Seasonal patterns in depth of water uptake under contrasting annual and perennial systems in the corn belt region of the midwestern us. Plant and Soil, 308(1), 69–92.

Auler, A. C., Miara, S., Pires, L. F., Fonseca, A. F. d., & Barth, G. (2014). Soil physico-hydrical properties resulting from the management in Integrated Production Systems. Revista Ciência Agronômica, 45(5), 976-989.

Bagarello, V., Di Prima, S., & Iovino, M. (2014). Comparing alternative algorithms to analyze the beerkan infiltration experiment. Soil Science Society of America Journal, 78(3), 724–736.

Bargués Tobella, A., Reese, H., Almaw, A., Bayala, J., Malmer, A., Laudon, H., & Ilstedt, U. (2014). The effect of trees on preferential flow and soil infiltrability in an agroforestry parkland in semiarid Burkina Faso. Water Resources Research, 50(4), 3342-3354.

Baributsa, D. N., Foster, E. F., Thelen, K. D., Kravchenko, A. N., Mutch, D. R., & Ngouajio, M. (2008). Corn and cover crop response to corn density in an interseeding system. Agronomy Journal, 100(4), 981-987.

Basche, A., & DeLonge, M. (2017). The impact of continuous living cover on soil hydrologic properties: A meta-analysis. Soil Science Society of America Journal. 81(5): 1179-1190..

Benegas, L., Ilstedt, U., Roupsard, O., Jones, J., & Malmer, A. (2014). Effects of trees on infiltrability and preferential flow in two contrasting agroecosystems in central america. Agriculture, Ecosystems & Environment, 183, 185-196.

Benjamin, J. (1993). Tillage effects on near-surface soil hydraulic properties. Soil and Tillage Research, 26(4), 277–288.

Beven, K., & Germann, P. (2013). Macropores and water flow in soils revisited. Water Resources Research, 49(6), 3071–3092.

Bhattacharyya, R., Prakash, V., Kundu, S., & Gupta, H. (2006). Effect of tillage and crop rotations on pore size distribution and soil hydraulic conductivity in sandy clay loam soil of the indian himalayas. Soil and Tillage Research, 86(2), 129–140.

Blanco-Canqui, H., Mikha, M. M., Presley, D. R., & Claassen, M. M. (2011). Addition of Cover Crops Enhances No-Till Potential for Improving Soil Physical Properties. Soil Science Society of America Journal, 75(4), 1471–1482.

Bond, R. D., & Harris, J. R. (1964). The influence of the microflora on the physical properties of

soils. I. Effects associated with filamentous algae and fungi. Soil Research, 2(1), 111–122.

Bouma, J. (1981). Soil morphology and preferential flow along macropores. Agricultural Water Management, 3(4), 235–250.

Bundt, M., Albrecht, A., Froidevaux, P., Blaser, P., & Flühler, H. (2000). Impact of Preferential Flow on Radionuclide Distribution in Soil. Environmental Science & Technology, 34(18), 3895–3899.

Bundt, M., Widmer, F., Pesaro, M., Zeyer, J., & Blaser, P. (2001). Preferential flow paths: biological 'hot spots' in soils. Soil Biology and Biochemistry, 33(6), 729–738.

Burket, J. Z., Hemphill, D. D., & Dick, R. P. (1997). Winter cover crops and nitrogen management in sweet corn and broccoli rotations. HortScience, 32(4), 664–668.

Calonego, J. C., Raphael, J. P., Rigon, J. P., de Oliveira Neto, L., & Rosolem, C. A. (2017). Soil compaction management and soybean yields with cover crops under no-till and occasional chiseling. European Journal of Agronomy, 85, 31–37.

Capurro, J. E. (2020). Cultivos de cobertura para soja y maiz (Tech. Rep.). Oliveros, Santa Fe, Argentina: EEA Oliveros, INTA.

Carter, M. R., & Gregorich, E. G. (2007). Soil sampling and methods of analysis. CRC press.

Castellano, M., & Valone, T. (2007). Livestock, soil compaction and water infiltration rate: Evaluating a potential desertification recovery mechanism. Journal of Arid Environments, 71, 97-108.

Chalise, K. S., Singh, S., Wegner, B. R., Kumar, S., Pérez-Gutiérrez, J. D., Osborne, S. L., ... Rohila, J. S. (2018). Cover crops and returning residue impact on soil organic carbon, bulk density, penetration resistance, water retention, infiltration, and soybean yield. Agronomy Jornal, 111(1), 99–108.

Clark, A. (2015). Cover crops for sustainable crop rotations. Grants and Education to Advance Innovations in Sustainable Agriculture (SARE).

Clark, G. A., & Smajstrla, A. G. (1993). Application volumes and wetting patterns for scheduling drip irrigation in florida vegetable production. Circular (USA).

Clothier, B., Sauer, T., & Scotter, D. (1991). Redistribution of Water and Solute Following Infiltration From a Surface Drip Source. Water Resources Research, 27, 2091-2097.

Cullum, R. (2009). Macropore flow estimations under no-till and till systems. Catena, 78(1), 87–91.

Czarnes, S., Hallett, P. D., Bengough, A. G., & Young, I. M. (2000). Root and microbial derived mucilages affect soil structure and water transport. European Journal of Soil Science, 51(3), 435-443.

Daigh, A. L., Helmers, M., Kladivko, E., Zhou, X., Goeken, R., Cavdini, J., ... Sawyer, J. (2014). Soil water during the drought of 2012 as affected by rye cover crops in fields in iowa and indiana. Journal of Soil and Water Conservation, 69(6), 564–573.

De Mendiburu, F. (2021). agricolae: Statistical procedures for agricultural research [Computer software manual]. (R package version 1.3-5)

De Baets, S., Poesen, J., Meersmans, J., & Serlet, L. (2011). Cover crops and their erosion-reducing effects during concentrated flow erosion. Catena, 85(3), 237–244.

De Rooij, G. H. (2000). Modeling fingered flow of water in soils owing to wetting front instability: a review. Journal of Hydrology, 231-232, 277–294.

Durner, W. (1992). Predicting the unsaturated hydraulic conductivity using multi-porosity water retention curves. Indirect methods for estimating the hydraulic properties of unsaturated soils, 185–202.

Fatehnia, M., Tawfiq, K., & Ye, M. (2016). Estimation of saturated hydraulic conductivity from double-ring infiltrometer measurements: Accurate estimation of hydraulic conductivity (ks) with DRI test data. European Journal of Soil Science, 67(2), 135–147.

Fenta, B. A., Schlüter, U., Garcia, B. M., DuPlessis, M., Foyer, C. H., & Kunert, K. J. (2011). Identification and application of phenotypic and molecular markers for abiotic stress tolerance in soybean. Soybean—Genetics and Novel Techniques for Yield Enhancement, 181–200.

Fernandez, R., Alvarez, C. O., Owen, E. R. E., & Quiroga, A. R. (2020). Effect of cover crop use on a continuous soybean sequence in the pampean semiarid region. Revista de la Facultad

de Agronomia, 30(2), 37-49.

Gardner, W. (1958). Some steady-state solutions of the unsaturated moisture flow equation with application to evaporation from a water table. Soil science, 85(4), 228–232.

Ghestem, M., Sidle, R. C., & Stokes, A. (2011). The Influence of Plant Root Systems on Subsurface Flow: Implications for Slope Stability. BioScience, 61(11), 869–879.

Gowdish, L. C., & Muñoz-Carpena, R. (2018). A transient quasi-3d point-source green-ampt infiltration and redistribution model. Vadose Zone Journal, 17(1), 180032.

Haghverdi, A., Najarchi, M., Öztürk, H. S., & Durner, W. (2020). Studying unimodal, bimodal, pdi and bimodal-pdi variants of multiple soil water retention models: I. direct model fit using the extended evaporation and dewpoint methods. Water, 12(3), 900.

Haruna, S., & Nkongolo, N. (2015). Cover Crop Management Effects on Soil Physical and Biological Properties. Procedia Environmental Sciences, 29, 13-14.

Haruna, S., Nkongolo, N., Anderson, S., Eivazi, F., & Zaibon, S. (2018). In situ infiltration as influenced by cover crop and tillage management. Journal of Soil and Water Conservation, 73(2), 164-172.

Hendrickx, J. M., & Flury, M. (2001). Uniform and preferential flow mechanisms in the vadose zone. Conceptual models of flow and transport in the fractured vadose zone, 149–187.

Hillel, D. (1998). Environmental soil physics: Fundamentals, applications, and environmental considerations. Elsevier.

Hinnell, A. C., Lazarovitch, N., & Warrick, A. W. (2009). Explicit infiltration function for boreholes under constant head conditions. Water Resources Research, 45(10).

Hinsinger, P., Bengough, A. G., Vetterlein, D., & Young, I. M. (2009). Rhizosphere: biophysics, biogeochemistry and ecological relevance. Plant and Soil, 321(1), 117–152.

Hubbard, R., Berdanier, C., Perkins, H., & Leonard, R. (1985). Characteristics of selected upland soils of the georgia coastal plain. ARS (USA).

Hubbard, R., Strickland, T., & Phatak, S. (2013). Effects of cover crop systems on soil physical properties and carbon/nitrogen relationships in the coastal plain of southeastern usa. Soil

and Tillage Research, 126, 276–283.

Jačka, L., Pavlásek, J., Kuráž, V., & Pech, P. (2014). A comparison of three measuring methods for estimating the saturated hydraulic conductivity in the shallow subsurface layer of mountain podzols. Geoderma, 219–220, 82–88.

Jarosław Kaszubkiewicz. (2015). Model for predicting the soil water retention curve. Institute of Soil Science and Environment Protection, University of Life Science, Wrocław,Poland. Unpublished.

Jiang, X. J., Chen, C., Zhu, X., Zakari, S., Singh, A. K., Zhang, W., ... Liu, W. (2019). Use of dye infiltration experiments and HYDRUS-3D to interpret preferential flow in soil in a rubber-based agroforestry systems in Xishuangbanna, China. Catena, 178, 120–131.

Jiang, X. J., Liu, W., Chen, C., Liu, J., Yuan, Z.-Q., Jin, B., & Yu, X. (2018). Effects of three morphometric features of roots on soil water flow behavior in three sites in China. Geoderma, 320, 161–171.

Jiang, X. J., Liu, W., Wu, J., Wang, P., Liu, C., & Yuan, Z.-Q. (2017). Land degradation controlled and mitigated by rubber based agroforestry systems through optimizing soil physical conditions and water supply mechanisms: A case study in xishuangbanna, china. Land Degradation & Development, 28(7), 2277-2289.

Jiang, X.-J., Zakari, S., Wu, J., Singh, A. K., Chen, C., Zhu, X., ... Liu, W. (2020). Can complementary preferential flow and non-preferential flow domains contribute to soil water supply for rubber plantation? Forest Ecology and Management, 461, 117948.

Johnson, J. M. F., Strock, J. S., Tallaksen, J. E., & Reese, M. H. (2016). Corn stover harvest changes soil hydrology and soil aggregation. Soil and Tillage Research, 161, 106–115.

Kahl, J. S., Fernandez, I. J., Rustad, L. E., & Peckenham, J. (1996). Threshold Application Rates of Wood Ash to an Acidic Forest Soil. Journal of Environmental Quality, 25(2), 220-227.

Katsura, S., Kosugi, K., Yamamoto, N., & Mizuyama, T. (2006). Saturated and Unsaturated Hydraulic Conductivities and Water Retention Characteristics of Weathered Granitic Bedrock. Vadose Zone Journal, 5(1), 35–47.

Lal, R., & Vandoren, D. (1990). Influence of 25 years of continuous corn production by three tillage methods on water infiltration for two soils in Ohio. Soil and Tillage Research, 16(1-2), 71–84.

Lassabatère, L., Angulo-Jaramillo, R., Ugalde, J. M. S., Cuenca, R., Braud, I., & Haverkamp, R. (2006). Beerkan Estimation of Soil Transfer Parameters through Infiltration Experiments—BEST. Soil Science Society of America Journal, 70(2), 521-532.

Lassabatère, L., Prima, S. D., Bouarafa, S., Iovino, M., Bagarello, V., & Angulo-Jaramillo, R. (2019). BEST-2K Method for Characterizing Dual-Permeability Unsaturated Soils with Ponded and Tension Infiltrometers. Vadose Zone Journal, 18(1), 180124.

Lenhard, R., Parker, J., & Mishra, S. (1989). On the correspondence between brooks-corey and van genuchten models. Journal of Irrigation and Drainage Engineering, 115(4), 744–751.

Ludwig, J. A., Wilcox, B. P., Breshears, D. D., Tongway, D. J., & Imeson, A. C. (2005). Vegetation Patches and Runoff–Erosion as Interacting Ecohydrological Processes in Semiarid Landscapes. Ecology, 86(2), 288–297.

Ma, Y., & Song, X. (2016). Using stable isotopes to determine seasonal variations in water uptake of summer maize under different fertilization treatments. Science of the Total Environment, 550, 471–483.

Marcillo, G., & Miguez, F. (2017). Corn yield response to winter cover crops: An updated meta-analysis. Journal of Soil and Water Conservation, 72(3), 226–239.

Mengel, D., & Barber, S. (1974). Development and distribution of the corn root system under field conditions 1. Agronomy Journal, 66(3), 341–344.

Niemeyer, R. J., Fremier, A. K., Heinse, R., Chávez, W., & DeClerck, F. J. (2014). Woody Vegetation Increases Saturated Hydraulic Conductivity in Dry Tropical Nicaragua. Vadose Zone Journal, 13(1).

Nofziger, D. L., & Wu, J. (2000). Soil physics teaching tools: Steady-state water movement in soils. Journal of Natural Resources and Life Sciences Education, 29(1), 130-134.

Owusu, G. (2015). vadose: The estimation of saturated hydraulic conductivity and soil water

retention curves in the vadose zone [Computer software manual]. (R package version 1.0-0)

R Core Team. (2022). R: A language and environment for statistical computing [Computer software manual]. Vienna, Austria.

Reynolds, W., Bowman, B., Brunke, R., Drury, C., & Tan, C. (2000). Comparison of tension infiltrometer, pressure infiltrometer, and soil core estimates of saturated hydraulic conductivity. Soil Science Society of America Journal, 64(2), 478–484.

Reynolds, W., & Elrick, D. (1991). Determination of hydraulic conductivity using a tension infiltrometer. Soil Science Society of America Journal, 55(3), 633–639.

Reynolds, W., Topp, G., & Vieira, S. (1992). An assessment of the single-head analysis for the constant head well permeameter. Canadian Journal of Soil Science, 72(4), 489–501.

Rezanezhad, F., Vogel, H.-J., & Roth, K. (2006). Experimental study of fingered flow through initially dry sand. Hydrology and Earth System Sciences Discussions, 3(4), 2595–2620.

Ritsema, C. J., & Dekker, L. W. (1995). Distribution flow: A general process in the top layer of water repellent soils. Water Resources Research, 31(5), 1187–1200.

Ritsema, C. J., Dekker, L. W., Elsen, E. G. M. V. D., Oostindie, K., Steenhuis, T. S., & Nieber, J. L. (1997). Recurring fingered flow pathways in a water repellent sandy field soil. Hydrology and Earth System Sciences, 1(4), 777–786.

Rönnqvist, H. (2018). Double-Ring Infiltrometer for In-Situ Permeability Determination of Dam Material. Engineering, 10, 320–328.

Rousseva, S., Kercheva, M., Shishkov, T., Lair, G. J., Nikolaidis, N., Moraetis, D., … others (2017). Soil water characteristics of european soiltrec critical zone observatories. Advances in agronomy, 142, 29–72.

Saxton, K. E., & Rawls, W. J. (2006). Soil Water Characteristic Estimates by Texture and Organic Matter for Hydrologic Solutions. Soil Science Society of America Journal, 70(5), 1569–1578.

Schulte, K., Culligan, P., & Germaine, J. (2007). Intrinsic Sorptivity and Water Infiltration into Dry Soil at Different Degrees of Saturation. Geotechnical Special Publication, 226.

Shukla, M. K. (2013). Soil physics: An introduction. CRC press.

Silva, A. L. B. R. d., Hashiguti, H. T., Zotarelli, L., Migliaccio, K. W., & Dukes, M. D. (2018). Soil Water Dynamics of Shallow Water Table Soils Cultivated With Potato Crop. Vadose Zone Journal, 17(1), 180077.

Šimůnek, J., van Genuchten, M. T., & Wendroth, O. (1998). Parameter Estimation Analysis of the Evaporation Method for Determining Soil Hydraulic Properties. Soil Science Society of America Journal, 62(4), 894–905.

Singer, J. W., & Meek, D. W. (2004). Repeated biomass removal affects soybean resource utilization and yield. Agronomy Journal, 96(5), 1382-1389.

Smettem, K., & Clothier, B. (1989). Measuring unsaturated sorptivity and hydraulic conductivity using multiple disc permeameters. Journal of Soil Science, 40(3), 563–568.

Snapp, S. S., Swinton, S. M., Labarta, R., Mutch, D., Black, J. R., Leep, R., ... O'neil, K. (2005). Evaluating cover crops for benefits, costs and performance within cropping system niches. Agronomy journal, 97(1), 322–332.

Sommer, R., & Stöckle, C. (2010). Correspondence between the campbell and van genuchten soil-water-retention models. Journal of irrigation and drainage engineering, 136(8), 559–562.

Thony, J., Vachaud, T., Clothier, B., & Angulo, J. (1991). Field measurement of the hydraulic properties of soil. Soil Technology. Vol 4, p. 111 - 123. Cremlingen. Germany..

Villamil, M., Bollero, G., Darmody, R., Simmons, F., & Bullock, D. (2006). No-till corn/soybean systems including winter cover crops: Effects on soil properties. Soil Science Society of America Journal, 70(6), 1936–1944.

Wang, R., & Strong, D. (1996). Beyond accuracy: What data quality means to data consumers. Journal of management information systems, 12(4), 5–33.

Wang, X., Chau, H., Si, B., Yao, N., Li, Y., & Wang, Y. (2018). Water movement and finger flow characterization in homogeneous water-repellent soils. Vadose Zone Journal, 17(1), 1–12.

Weiler, M., & Flühler, H. (2004). Inferring flow types from dye patterns in macroporous soils. Geoderma, 120(1), 137–153.

White, I., Sully, M. J., & Perroux, K. M. (1992). Measurement of surface-soil hydraulic properties: Disk permeameters, tension infiltrometers, and other techniques. Advances in measurement of soil physical properties: Bringing theory into practice, 30, 69–103.

William, S., & Roth, W. (2017). Cover crop interseeder: Impacts on corn yield. The agriculture extension magazine.

Wine, M. L., Ochsner, T. E., Sutradhar, A., & Pepin, R. (2012). Effects of eastern red-cedar encroachment on soil hydraulic properties along Oklahoma's grassland-forest ecotone. Hydrological Processes, 26(11), 1720–1728.

Wooding, R. (1968). Steady infiltration from a shallow circular pond. Water resources research, 4(6), 1259–1273.

Yang, X., Fan, J., & Jones, S. B. (2018). Effect of Soil Texture on Estimates of Soil-Column Carbon Dioxide Flux Comparing Chamber and Gradient Methods. Vadose Zone Journal, 17(1), 180112.

Yilmaz, D., Lassabatere, L., Angulo-Jaramillo, R., Deneele, D., & Legret, M. (2010). Hydrodynamic characterization of basic oxygen furnace slag through an adapted best method. Vadose Zone Journal, 9(1), 107–116.

Zhu, X., Chen, C., Wu, J., Yang, J., Zhang, W., Zou, X., ... Jiang, X. (2019). Can intercrops improve soil water infiltrability and preferential flow in rubber-based agroforestry system? Soil and Tillage Research, 191, 327–339.

Zhuang, L., Hassanizadeh, S. M., Duijn, C. J. v., Zimmermann, S., Zizina, I., & Helmig, R. (2019). Experimental and Numerical Studies of Saturation Overshoot during Infiltration into a Dry Soil. Vadose Zone Journal, 18(1), 180167.

Zumr, D., Jeřábek, J., Klípa, V., Dohnal, M., & Sněhota, M. (2019). Estimates of tillage and rainfall effects on unsaturated hydraulic conductivity in a small central european agricultural catchment. Water, 11(4), 740.

Zwartendijk, B., van Meerveld, I., Ghimire, C., Bruijnzeel, L., Ravelona, M., & Jones, J. (2017). Rebuilding soil hydrological functioning after swidden agriculture in eastern Madagascar.

Agriculture, Ecosystems & Environment, 239, 101–111.